The Journal of Immunology

B Cell–Intrinsic TLR7 Signaling Is Essential for the Development of Spontaneous Germinal Centers

Chetna Soni, Eric B. Wong, Phillip P. Domeier, Tahsin N. Khan, Takashi Satoh, Shizuo Akira and Ziaur S. M. Rahman

J Immunol 2014; 193:4400-4414; Prepublished online 24 September 2014;
doi: 10.4049/jimmunol.1401720
http://www.jimmunol.org/content/193/9/4400

The Journal of Immunology is published twice each month by
The American Association of Immunologists, Inc.,
1451 Rockville Pike, Suite 650, Rockville, MD 20852

Print ISSN: 0022-1767 Online ISSN: 1550-6606.

B Cell–Intrinsic TLR7 Signaling Is Essential for the Development of Spontaneous Germinal Centers

Chetna Soni,*,[1] Eric B. Wong,*,[1] Phillip P. Domeier,* Tahsin N. Khan,*,† Takashi Satoh,‡ Shizuo Akira,‡ and Ziaur S. M. Rahman*

Spontaneous germinal center (Spt-GC) B cells and follicular helper T cells generate high-affinity autoantibodies that are involved in the development of systemic lupus erythematosus. TLRs play a pivotal role in systemic lupus erythematosus pathogenesis. Although previous studies focused on the B cell–intrinsic role of TLR-MyD88 signaling on immune activation, autoantibody repertoire, and systemic inflammation, the mechanisms by which TLRs control the formation of Spt-GCs remain unclear. Using nonautoimmune C57BL/6 (B6) mice deficient in MyD88, TLR2, TLR3, TLR4, TLR7, or TLR9, we identified B cell–intrinsic TLR7 signaling as a prerequisite to Spt-GC formation without the confounding effects of autoimmune susceptibility genes and the overexpression of TLRs. TLR7 deficiency also rendered autoimmune B6.*Sle1b* mice unable to form Spt-GCs, leading to markedly decreased autoantibodies. Conversely, B6.*yaa* and B6.*Sle1b.yaa* mice expressing an extra copy of TLR7 and B6.*Sle1b* mice treated with a TLR7 agonist had increased Spt-GCs and follicular helper T cells. Further, TLR7/MyD88 deficiency led to compromised B cell proliferation and survival after B cell stimulation both in vitro and in vivo. In contrast, TLR9 inhibited Spt-GC development. Our findings demonstrate an absolute requirement for TLR7 and a negative regulatory function for TLR9 in Spt-GC formation under nonautoimmune and autoimmune conditions. Our data suggest that, under nonautoimmune conditions, Spt-GCs initiated by TLR7 produce protective Abs. However, in the presence of autoimmune susceptibility genes, TLR7-dependent Spt-GCs produce pathogenic autoantibodies. Thus, a single copy of TLR7 in B cells is the minimal requirement for breaking the GC-tolerance checkpoint. ***The Journal of Immunology*****, 2014, 193: 4400–4414.**

Upon T cell–dependent antigenic stimulation, B cells differentiate into either preplasma IgM^+ recirculating memory B cells or extrafollicular Ab-forming cells (AFCs) or they form germinal centers (GCs) within primary follicles (1, 2). Extrafollicular AFCs are generally short-lived and secrete IgM and/or low-affinity class-switched Abs. In contrast, rapidly dividing GC B cells undergo class-switch recombination and site-directed somatic hypermutation of their Ig V region genes (3, 4). Clones selected for increased Ag affinity survive and differentiate into Ab-producing long-lived plasma cells or memory B cells (4). Many of the GC-derived, long-lived plasma cells home to the bone marrow (BM) and produce high-affinity Abs, conferring lasting humoral immunity (5–7).

B cells have emerged as key players in TLR-mediated systemic autoimmune responses, especially in systemic lupus erythematosus (SLE). Exposure of murine B cells to TLR4, TLR7, and TLR9 agonists increases the expression of B cell costimulatory factors and induces B cells to proliferate, produce cytokines, differentiate into APCs, switch Ig classes, and secrete Igs (8, 9). Consensus views drawn from studies on TLR7- and TLR9-dependent MyD88 signaling in autoimmune lupus-prone mouse models propose that TLR7 promotes inflammation and lupus pathogenesis, whereas TLR9 plays a negative-regulatory role to dampen the disease process (10–14). However, most of these studies focused primarily on the involvement of MyD88 or the two TLRs in B cell activation, autoantibody specificity, and the development of glomerulonephritis (11, 12, 15–20).

The GC is an important B cell–tolerance checkpoint in the periphery (21, 22). Several autoimmune-prone mice develop spontaneous GCs (Spt-GCs) in the spleen by 1–2 mo of age (23). Dysregulated GC B cell and follicular (FO) helper T cell (Tfh cell) responses make decisive contributions to the generation of class-switched autoantibodies and to the development of lupus in mouse models (22, 24–26), as well as to human SLE (27, 28). We also recently reported a strong correlation between autoantibody production and Spt-GCs in B6.*Sle1b* mice harboring the lupus-associated SLAM genes derived from the autoimmune NZM2410 strain (29). Understanding altered regulation of both the FO GC and extrafollicular pathways by TLRs in autoimmune diseases will help to develop treatment options for the heterogeneous population of SLE patients in whom either or both pathways may be affected. Earlier studies extensively investigated the involvement of TLRs in modulating autoimmune responses using MRL/lpr mice (11, 15). This model allows for the extrafollicular differentiation of B cells (15, 30). Recently, using different TLR-overexpression and knockout (KO) autoimmune mouse models, several groups suggested B cell–intrinsic and/or -extrinsic roles

*Department of Microbiology and Immunology, Pennsylvania State University College of Medicine, Hershey, PA 17033; †Department of Molecular Microbiology and Immunology, Oregon Health and Science University, Portland, OR 97239; and ‡Department of Host Defense, Research Institute for Microbial Diseases, Osaka University, Osaka 565-0871, Japan

[1]C.S. and E.B.W. contributed equally to this work.

Received for publication July 8, 2014. Accepted for publication August 28, 2014.

This work was supported by National Institutes of Health Grant AI091670 (to Z.S.M.R.).

Address correspondence and reprint requests to Dr. Ziaur Rahman, Department of Microbiology and Immunology, H107, Pennsylvania State University College of Medicine, 500 University Drive, Hershey, PA 17033-0850. E-mail address: zrahman@hmc.psu.edu

The online version of this article contains supplemental material.

Abbreviations used in this article: AFC, Ab-forming cell; ANA, anti-nuclear Ab; AP, alkaline phosphatase; B6, C57BL/6; BAFF, B cell activating factor; BM, bone marrow; DC, dendritic cell; FDC, FO dendritic cell; FO, follicular; GC, germinal center; IMQ, imiquimod; KO, knockout; MZ, marginal zone; PI, propidium iodide; PNA, peanut agglutinin; SA, streptavidin; SLE, systemic lupus erythematosus; Sm/RNP, Smith Ag/ribonucleoprotein; Spt-GC, spontaneous GC; Tfh cell, follicular helper T cell.

for TLR-MyD88 signaling in the GC-differentiation pathway of autoantibody production and autoimmune inflammatory responses (20, 31–33). However, the mechanisms and the requirement for physiological levels of individual TLRs in controlling the formation of Spt-GCs and Tfh cell development remain unclear.

In this study, we first addressed the requirement for TLRs in the development of Spt-GC B cells and Tfh cells in the steady-state. These studies were performed under nonautoimmune conditions, without the confounding effects of TLR overexpression, exogenous TLR stimulation, or purposeful immunizations. We found that B cell–intrinsic TLR7-MyD88 signaling was required for the formation of Spt-GCs and that TLR9 signaling negatively regulated the magnitude of the TLR7-mediated response. In agreement with our observations in nonautoimmune mice, TLR7-deficient autoimmune B6.*Sle1b* mice (*Sle1b*/TLR7-KO) also were unable to initiate GC formation, even by 6 mo of age, and they had diminished total Ab and autoantibody responses. Our ex vivo and in vivo studies indicated suboptimal B cell survival and proliferation in the absence of TLR7. These results highlight the absolute requirement for TLR7 and the negative-regulatory function of TLR9 in Spt-GC responses in nonautoimmune and autoimmune environments.

Materials and Methods

Mice

C57BL/6 (B6) mice, 3 mo of age (for particular experiments), were purchased from The Jackson Laboratory (Bar Harbor, ME), Taconic (Hudson, NY), Charles River (Wilmington, MA), or the National Cancer Institute (Bethesda, MD). Spleens from B6 mice, housed at The Rockefeller University (New York, NY) germ-free facility and specific pathogen–free facility, were kindly provided by Dr. Daniel Mucida. MyD88$^{fl/fl}$, CD11c-Cre$^{+/-}$-MyD88$^{fl/fl}$, and LysM-Cre$^{+/-}$-MyD88$^{fl/fl}$ mice were a kind gift from Dr. Milena Bogunovic (Pennsylvania State University College of Medicine, Hershey, PA). Breeding pairs for B6, B6.μMT (B6.129S2-*Ighm*^{tm1Cgn}/J), Rag1-KO, B6.SB-*yaa*/J (B6.*yaa*), MyD88-KO [B6.129P2(SJL)-*Myd88*$^{tm1.1Defr}$/J], and OT-II–transgenic [B6.Cg-Tg (TcraTcrb)425Cbn/J] mice were originally purchased from The Jackson Laboratory and bred in-house. TLR7-KO (34) and TLR9-KO (35) mice backcrossed to B6 mice for 10 generations were bred in-house. The derivation of B6 mice congenic for the *Sle1b* sublocus (named B6.*Sle1b*) was described previously (36). B6.*Sle1b.yaa* mice were generated by breeding B6.*yaa* males with B6.*Sle1b* females. *Sle1b*/TLR7-KO and *Sle1b*/TLR9-KO mice were generated by crossing B6.*Sle1b* mice with TLR7-KO and TLR9-KO lines, respectively. All animals were housed in the specific pathogen–free animal facility at Pennsylvania State University College of Medicine, and all procedures were performed in accordance with the guidelines approved by the Pennsylvania State University Institutional Animal Care and Use Committee.

Flow cytometry

The following Abs were used for flow cytometric analysis of mouse splenocytes or BM cells. PacBlue–anti-B220 (RA3-6B2), Alexa Fluor 700–anti-CD4 (RM4-5), PE–anti-PD-1 (29F.1A12), PerCP–Cy5.5–anti-CD69 (H1.2F3), allophycocyanin–anti-TCR Vα2 (B20.1), allophycocyanin–Cy7–anti-CD25 (PC61), Cy5–anti-CD86 (GL1), PeCy7–anti-CD95 (FAS, Jo2), PeCy7–anti-MHC II (M5/114.15.2), allophycocyanin–anti-CD24 (HSA) (M1/69), biotin–anti-Ly5.1 (BP-1) (6C3), FITC–anti-CD23 (B3B4), and PE-Cy5–streptavidin (SA) were from purchased from BioLegend (San Diego, CA). Biotin–anti-CXCR5 (2G8), FITC–anti-CD11c (HL3), FITC–anti-CD43 (S7) were from BD Pharmingen (San Diego, CA). FITC–peanut agglutinin (PNA) was from Vector Labs (Burlingame, CA). PE–anti-IgM (eB121-15F9), allophycocyanin–anti-CD93 (AA4.1), and FITC–anti-F4/80 (BM8) were from eBioscience (San Diego, CA). Stained cells were analyzed using a BD LSR II flow cytometer (BD Biosciences, Franklin Lakes, NJ). Data were acquired using FACSDiva software (BD Biosciences, San Jose, CA) and analyzed using FlowJo software (TreeStar, San Carlos, CA). Dead cells were quantified by flow cytometry using DAPI (Sigma-Aldrich, St. Louis, MO).

Histology, immunofluorescence, and anti-nuclear Ab staining

The following Abs and reagents were used for immunohistochemical analysis of mouse spleen sections: biotin-mouse anti-rat IgG (Jackson ImmunoResearch, West Grove, PA); alkaline phosphatase (AP)-SA, Vector Blue AP Substrate Kit III, and Vector NovaRED Substrate Kit (all from Vector Labs); HRP-PNA (Sigma-Aldrich); and biotin–anti-IgD (11-26; Southern Biotechnology Associates). Immunofluorescence staining Abs, including anti-mouse Ki67 (16A8BL; BioLegend); PE–anti-CD4 (GK1.5), FITC-GL7 (RA3-6B2), purified rat anti-mouse FDC-M1, and allophycocyanin–anti-IgD, were from BD Biosciences (Franklin Lakes, NJ). FITC–anti-CD35 (eBio4E3) was from eBioscience. Biotin–anti-MFG-E8 (18A2-G10) was from MBL (Naka-ku-Nagoya, Japan). Kidney sections were stained for C3 using FITC–anti-C3 from Immunology Consultants Laboratory (Portland, OR). Anti-nuclear Abs (ANAs) were detected by indirect immunofluorescence staining of Hep-2 culture slides (Antibodies, Davis, CA) using serum from mice at a 1:50 dilution in PBS, probed with FITC–rat anti-mouse κ (H139-52.1; Southern Biotechnologies Associates, Birmingham, AL). For imaging spleen sections, we used a Leica DM4000 microscope and Leica software (LAS-AF) (Leica Microsystems, Buffalo Grove, IL). The color intensity of images was enhanced slightly using Adobe Photoshop CS4 (Adobe Systems, San Jose, CA). This was necessary for better visualization and was carried out consistently between control and test sections while maintaining the integrity of the data.

ELISPOT assays

ELISPOT assays were performed as described (37). Briefly, splenocytes in 10% RPMI 1640 with antibiotics were plated at a concentration of 1×10^5 cells/well onto anti-IgM–coated or anti-IgG–coated (Invitrogen, Grand Island, NY) multiscreen 96-well filtration plates (Millipore, Bedford, MA) or at 1×10^6 cells/well on dsDNA-, histone-, or nucleosome-coated multiscreen 96-well filtration plates. Serially diluted (1:2) cells were incubated for 6 h at 37°C. IgM-producing AFCs were detected using biotinylated anti-mouse IgM (Jackson ImmunoResearch) and SA-AP (Vector Labs). IgG-producing AFCs were detected using AP-conjugated anti-mouse IgG (Molecular Probes, Grand Island, NY). dsDNA-, histone-, and nucleosome-specific AFCs were detected by biotinylated anti-κ Ab (Invitrogen) and SA-AP (Vector Labs). Plates were developed using the Vector Blue AP Substrate Kit III (Vector Labs). ELISPOTs were counted and analyzed using a computerized imaging/analysis system (Cellular Technology, Shaker Heights, OH).

Serology: Ig and autoantibody titers

Total serum IgM/IgG or IgG from in vitro B cell culture supernatants was measured using standard ELISA protocols. Serum Ab titers were quantitated as described (29). Briefly, ELISA plates were coated with anti-IgM or anti-IgG capture Abs (Invitrogen) and detected using biotinylated anti-mouse IgM (Jackson ImmunoResearch) or AP-conjugated anti-mouse IgG (Molecular Probes). Total IgG autoantibody titers were measured in ELISA plates coated with dsDNA, histone, nucleosome, Smith Ag/ribonucleoprotein (Sm/RNP), or cardiolipin and detected with biotinylated anti-κ Ab (Invitrogen). IgG subtype–specific autoantibody titers were detected by biotinylated IgG1, biotinylated IgG2b, and AP-IgG2c Abs (Southern Biotech). Biotinylated Abs were detected by SA-AP (Vector Labs). The plates were developed by p-Nitrophenyl Phosphate, Disodium Salt (Thermo Fisher Scientific, Rockford, IL) substrates for AP.

Generation of BM chimeric mice

Ten- to twelve-week-old female B6.μMT mice (recipients) were lethally irradiated with 1000 rad x-rays (X-Rad 320iX Research Irradiator; Precision X-Ray, North Branford, CT) prior to the transfer of BM cells. Each mouse received 7–10 $\times 10^6$ (T cell–depleted) BM cells (i.v.) isolated from 8–10-wk-old female donor mice, with 80% cells from B6.μMT mice and 20% cells from B6, TLR9-KO, or TLR7-KO mice. The recipient mice were analyzed after 3 mo for Spt-GC B cells and Tfh cells.

Adoptive transfer

CD4$^+$ T cells were purified by negative selection from B6 mice using a mouse *Pan* T Cell Isolation Kit II (Miltenyi Biotec, Bergisch Gladbach, Germany). B cells from B6, TLR7-KO, or TLR9-KO mice were negatively selected using anti-CD43 (Ly-48) MicroBeads (Miltenyi Biotec). Purified B and T cells were mixed at a 3:1 ratio and transferred (i.v.) into Rag1-KO mice. Two months later, mice were sacrificed, and spleens were analyzed for Spt-GCs.

In vitro B cell–proliferation assay

B cells were purified from naive 8–10-wk-old B6, TLR7-KO, TLR9-KO, or MyD88-KO mice with mouse anti-CD43 (Ly-48) MicroBeads. Purified B cells were stained with 3 μM CFSE (Sigma Aldrich) in PBS with 5% FBS for 15 min at room temperature. Stained B cells were cultured with 25 μg/ml soluble anti-IgM (Jackson ImmunoResearch) and 20 μg/ml soluble

anti-CD40 Ab (BioLegend), with or without 10 ng/ml B cell activating factor (BAFF; PeproTech, Rocky Hill, NJ). After 72 or 96 h of stimulation, cells were surface stained (if required), DAPI stained or fixed, and subjected to flow cytometry.

In vivo B cell proliferation

Eight- to ten-week-old female B6.μMT mice were immunized with 200 μl 10% SRBCs in PBS, 2 d prior to cell transfers. Each mouse received (i.v.) 5×10^6 CFSE-labeled purified B cells from female B6, TLR7-KO, or TLR9-KO mice. Recipients were analyzed for B cell proliferation on the fourth day of transfer.

Cell cycle analysis

B cells were cultured with anti-IgM (25 μg/ml) and anti-CD40 (20 μg/ml) for the indicated time periods. Subsequently, cells were harvested and washed with chilled PBS and then fixed with chilled 70% ethanol overnight at −20°C. Cells were centrifuged at 1000 × *g* for 10 min at 4°C and washed with PBS. Propidium iodide (PI) staining solution containing 50 μg/ml PI, 50 μg/ml RNase A (Roche Applied Sciences, Indianapolis, IN), and 100 μM EDTA in PBS was used to stain the samples for 1–2 h at 42°C. Data were analyzed by flow cytometry.

RNA preparation and real-time RT-PCR

Total RNA was isolated using TRIzol reagent (Ambion, Grand Island, NY), as per the manufacturer's instructions, from total splenocytes or purified B cells of indicated mice. RNA was reverse transcribed using a high-capacity reverse transcription kit (Applied Biosystems, Grand Island, NY). Gene expression was quantified using a Power SYBR Green PCR Master Mix Kit and the StepOnePlus Real-Time PCR System (both from Applied Biosystems). Primers were designed using Primer3 software and synthesized by IDT Technologies (Coralville, IA). Amplification conditions for all primer sets were one cycle of 95°C for 10 min, followed by 40 cycles of 95°C for 15 s and 60°C for 1 min. 18srRNA was used as the reference gene for sample normalization. PCR primer sequences are as follows: PD-1 Forward 5′-GAG CTC GTG GTA ACA GAG AGA A-3′; PD-1 Reverse 5′-ACA GGG ATA CCC ACT AGG GC-3′: ICOS Forward 5′-CGG ATC CAG TGT GCA TGA CC-3′; ICOS Reverse 5′-AGC TTA TGA GGT CAC ACC TGC-3′: XBP-1 Forward 5′-GGC CAA GGG GAG TGG AGT AAG-3′; XBP-1 Reverse 5′-GCT GCA GAG GTG CAC ATA GTC-3′: IRF-4 Forward 5′-CAC AGC TCA TGT GGA ACC TCT-3′; IRF-4 Reverse 5′-TCA GGT AAC TCG TAG CCC CT-3′: Bcl-6 Forward 5′-AGA CAT TGG CAG AGT TCC AGA-3′; Bcl-6 Reverse 5′-CTG GCA GCG ATC ACA TTT GTA-3′: AICDA Forward 5′-CCT TCG CAA CAA GTC TGG CT-3′; AICDA Reverse 5′-GAA CCA GGT GAC GCG GTA A-3′; 18srRNA forward 5′-CAC TTT TGG GGC CTT CGT GT-3′; and 18srRNA Reverse 5′-AGG CCC AGA GAC TCA TTT CTT C-3′.

Statistical analysis

An unpaired, nonparametric, Mann–Whitney, Student *t* test was used to compare two groups, whereas one-way ANOVA, followed by the Tukey multiple-comparison test, was used to compare more than two groups. GraphPad Prism 6 software (La Jolla, CA) was used for all analyses. Error bars reflect mean, unless otherwise indicated. If the statistical analysis is not shown, nonsignificant differences were found.

Results

TLR7 drives the formation of steady-state Spt-GCs and Abs in B6 mice

GCs are usually described in the context of T-dependent antigenic stimulation or under autoimmune conditions (23, 38, 39). However, we observed Spt-GCs in unmanipulated, nonautoimmune B6 mice at 3 mo of age and older, housed in a specific pathogen–free facility, albeit at a lower frequency compared with age-matched autoimmune prone mice (29). We extended this observation to B6 mice housed in various facilities (The Jackson Laboratory, National Cancer Institute, Charles River, and Taconic) and found that, irrespective of the facility, all B6 mice developed well-defined Spt-GCs with comparable percentages of $B220^+PNA^{hi}Fas^{hi}$ GC B cells and $CD4^+CXCR5^{hi}PD\text{-}1^{hi}$ Tfh cells at ∼3 mo of age (data not shown).

Self-Ags and/or endogenous microbial components might stimulate TLRs, thereby driving the Spt-GC reaction (40–42). We compared Spt-GC B cell and Tfh cell percentages, in the absence of exogenous TLR stimulation, in 3-mo-old TLR2-, TLR3-, TLR4-, TLR7-, or TLR9-deficient mice with those in age- and sex-matched B6 mice. The percentages of Spt-GC B cells and Tfh cells in TLR2- and TLR3-deficient mice were comparable to B6 controls (Supplemental Fig. 1A, 1B). Although not statistically significant, TLR4-KO mice had lower percentages of Spt-GC B cells and Tfh cells compared with B6, TLR2-KO, and TLR3-KO mice (Supplemental Fig. 1A, 1B). However, histological analysis of 3-mo-old TLR4-KO spleens showed well-formed IgD^-GL7^+ GCs (Supplemental Fig. 1C), indicating that TLR4 is not required for the formation of Spt-GCs. At 3 mo of age, TLR7-KO mice had the lowest percentage of GC B cells and Tfh cells compared with B6 controls, although the difference was not statistically significant (Fig. 1A–D). However, at 6 mo, the percentage of GC B cells and Tfh cells was significantly reduced in TLR7-KO mice compared with B6 controls and TLR9-KO mice (Fig. 1E, 1F). Conversely, TLR9-KO mice had an increased percentage of GC B cells and Tfh cells compared with B6 and TLR7-KO mice starting at 3 mo of age (Fig. 1A–D). At 6 mo, the percentage of GC B cells in TLR9-KO mice was comparable to B6 mice; however, the Tfh cell percentage remained significantly elevated (Fig. 1E, 1F).

Immunohistological analysis of spleen sections from 3- and 6-mo-old mice revealed the complete absence of IgD^-PNA^+ Spt-GC B cells in TLR7-KO mice, whereas TLR9-KO mice had larger Spt-GCs than did B6 controls (Fig. 1G). Moreover, IgM- and IgG-producing AFCs were barely detected in TLR7-KO mice, whereas TLR9-KO mice exhibited a significant increase (Fig. 1H, 1I). TLR7-KO mice had significantly lower Ab titers of total serum IgG2b and IgG2c than did TLR9-KO mice (Fig. 1J). Average serum IgG2b and IgG2c titers in TLR7-KO mice were lower than in B6 controls, but the differences were not statistically significant (Fig. 1J). No significant differences were observed in IgM, total IgG, and IgG1 serum Ab titers among these three strains of mice (Fig. 1J). To ascertain whether the loss of Spt-GCs in TLR7-KO mice involved signaling via MyD88, we analyzed 3-mo-old MyD88-KO mice and found that they also were unable to develop Spt-GCs in the absence of antigenic stimulation compared with 3-mo-old B6 mice (Supplemental Fig. 1D).

To investigate the source of the TLR ligands stimulating Spt-GC formation in naive B6 mice, we treated B6 mice with antibiotics for 6 wk and compared their Spt-GC profile with control mice. We did not observe any effect of antibiotics treatment on the percentage of Spt-GC B cells or Tfh cells (Supplemental Fig. 1E, 1F). We also analyzed the Spt-GC profile of B6 germ-free mice and found that they also formed Spt-GCs, albeit to a reduced extent (Supplemental Fig. 1G), similar to TLR4-KO mice. These results suggest that TLR7 ligands (self-nucleic acids and/or retroviral elements) are the primary stimulators for the formation of Spt-GCs and Tfh cells (41, 43–45), whereas TLR4 ligands (endogenous microbial components) may have a role in maintaining GCs. These observations are consistent with the recent report by Giltiay et al. (46). They used mice expressing both TLR7 and RNase transgenes to show that self-RNA is involved in the anti-RNA Ab responses.

Markedly reduced Spt-GCs and Ab responses in TLR7-KO mice are not the outcome of developmental defects in primary B cells and FO dendritic cell network

Next, we tested whether markedly reduced Spt-GCs and Tfh cells in TLR7-KO mice resulted from a defect in primary B cell development and maturation in the absence of TLR7. Flow cytometric analysis of BM cells and splenocytes from B6, TLR9-KO, and TLR7-KO mice revealed no significant differences in the distribution of cells among

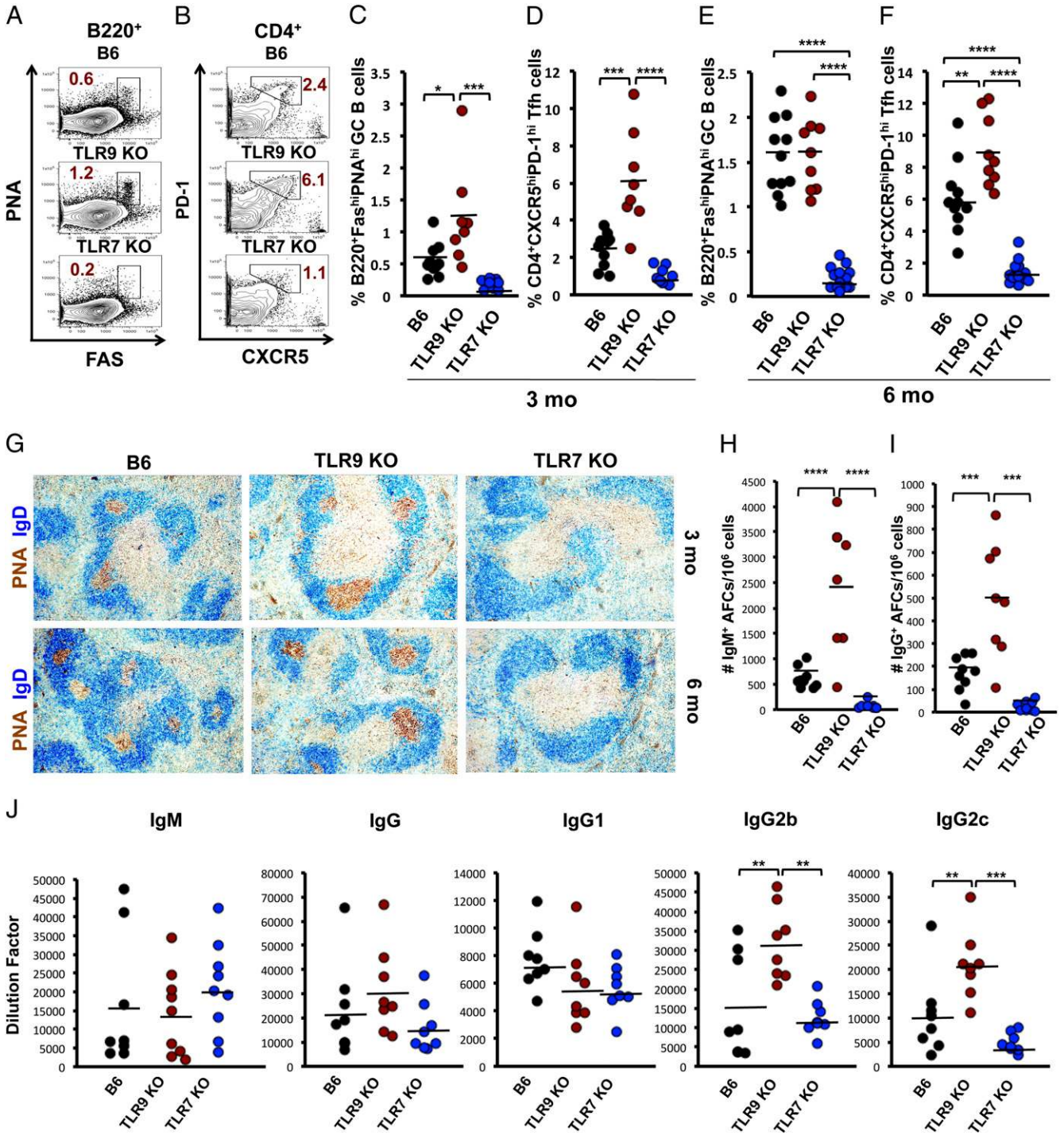

FIGURE 1. TLR7 is essential for Spt-GC formation in B6 mice. Gating strategy for GC B cells ($B220^+PNA^{hi}CD95^{hi}$) (**A**) and Tfh cells ($CD4^+CXCR5^{hi}$ $PD\text{-}1^{hi}$) (**B**). Percentage of GC B cells (**C**) and Tfh cells (**D**) at 3 mo of age. Percentage of GC B cells (**E**) and Tfh cells (**F**) at 6 mo of age. (**G**) Representative immunohistological analysis of spleen sections from three or four mice from each indicated group and age stained with GC B cell marker PNA (brown) and FO B cell marker IgD (blue). Original magnification ×100. ELISPOT analysis of IgM^+ (**H**) and IgG^+ (**I**) AFCs at 6 mo of age. (**J**) Total anti-IgM–specific, anti-IgG–specific, anti-IgG1–specific, anti-IgG2b–specific, and anti-IgG2c–specific serum Ab titers at 6 mo of age. Each circle represents an individual mouse. $*p \leq 0.05$, $**p \leq 0.01$, $***p \leq 0.001$, $****p \leq 0.0001$.

various B cell subsets in BM cells among the three strains of mice (Fig. 2A–D), fraction A being the most immature to the mature B cells in fraction F (47). We did not observe any significant differences in transitional type 1 (T1), type 2 (T2), type 3 (T3) (Fig. 2E), FO, or marginal zone (MZ) B cell populations in splenocytes (48) (Fig. 2F). Also, no discernible difference was observed in the expression of the maturation (IgD, CD23, and CD62L) and activation (CD69, CD80, and CD86) markers on B cells among all three strains of mice (data not shown). Immunohistochemistry further confirmed the presence of IgD^+ mature FO B cells in TLR7-KO spleens, which was comparable to B6 and TLR9-KO mice (Fig. 1G). Additionally, we measured Ca^{2+} flux in B cells upon BCR stimulation with anti-IgM Ab and observed no differences among B6, TLR7-KO, and TLR9-KO mice (data not shown).

We further examined whether TLR7 deficiency affected the primary development of stromal elements, such as FO dendritic

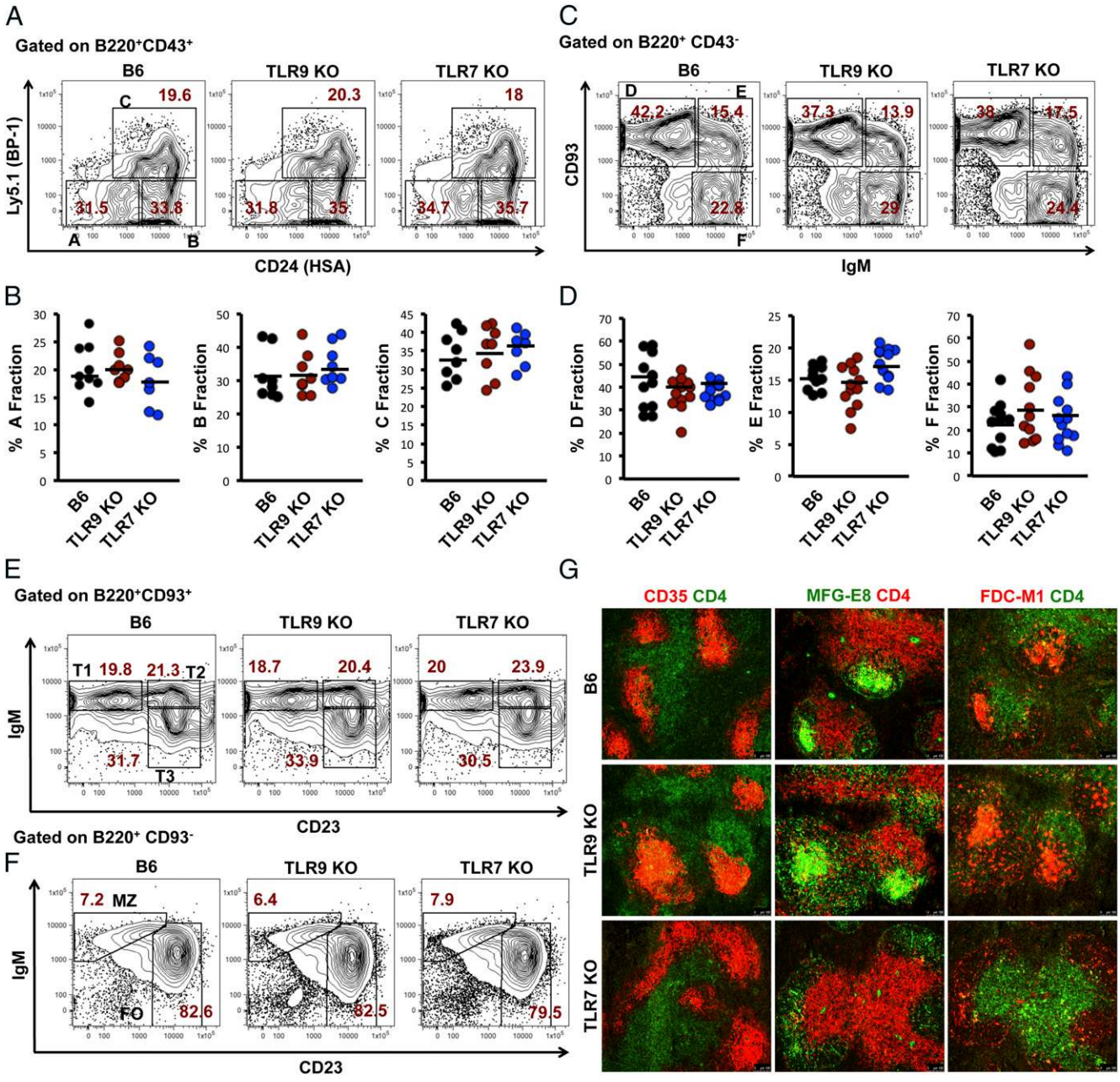

FIGURE 2. BM and splenic B cell and FDC development are normal in TLR7-KO mice. Representative contour plots show the gating strategy for the BM B cell developmental fractions A–C (**A**) and D–F (**C**). Scatter plots show the percentage of total BM cells from the indicated mice in fractions A–C (**B**) and D–F (**D**). Each circle represents an individual mouse. (**E**) Representative contour plots show the gating strategy and the percentage of splenic transitional type 1 (T1), type 2 (T2), and type 3 (T3) B cells. (**F**) Representative contour plots show gating strategy and percentage of MZ and FO B cells in total splenocytes of the indicated mice. (**G**) Representative immunofluorescence analysis of spleen sections from 6-mo-old mice stained for FDC markers (CD35, MFGE-8, FDC-M1) plus CD4. Flow cytometry data are representative of three or four independent experiments with three or four mice/group. Immunofluorescence data are representative of at least three or four mice/genotype. Original magnification ×100.

cells (FDCs), which are instrumental in the development of B cell follicles and the formation of GCs. Spleen sections from 6-mo-old B6, TLR9-KO, and TLR7-KO mice that were stained with anti-CD35 and anti-CD4 showed a comparable primary FO stromal network or FDCs (Fig. 2G). However, markers expressed on "secondary" FDCs during active formation of GCs, like MFG-E8 and FDC-M1, showed reduced expression in TLR7-KO mice compared with B6 and TLR9-KO mice, presumably due to the absence of Spt-GC formation (Fig. 2G). Together, these data demonstrated that a defect in primary B cell and FDC network development did not cause the complete absence of Spt-GCs in TLR7-KO mice.

*TLR7 promotes and TLR9 suppresses Spt-GC formation in autoimmune B6.*Sle1b *mice*

TLR7 has a pathogenic role and TLR9 has a protective function in murine SLE disease (10, 11, 13–15, 17, 49). Overexpression of TLR7 in mouse models suggested its role in the enhancement of GC and plasmablast development (32), whereas, low copy number of TLR7 expression did not have any effect on GC and plasma cell development (31). Recently, Jackson et al. (20) suggested opposing regulatory roles for B cell–specific TLR7 and TLR9 in GC and Tfh cell responses in a mouse model of systemic autoimmunity driven by mutations in WASp. We recently showed that

B6.*Sle1b* mice carrying lupus-associated SLAM family genes have significantly higher numbers of Spt-GC B cells and Tfh cells (29). However, the mechanism by which TLR7 and TLR9 may regulate Spt-GC formation and Tfh cell development in B6.*Sle1b* mice is not defined. To investigate, we generated TLR7-deficient (Sle1b/TLR7-KO) or TLR9-deficient (Sle1b/TLR9-KO) mice on the B6.*Sle1b* autoimmune genetic background. B6.*Sle1b* mice carry lupus-associated SLAM family genes (50), and B6.*Sle1b* females develop significantly higher numbers of Spt-GC B cells and Tfh cells than do B6 controls, leading to increased AFCs and ANAs (29).

Six-month-old female *Sle1b*/TLR7-KO mice failed to form Spt-GC B cells and Tfh cells compared with B6.*Sle1b* counterparts, which had an average of 3% Spt-GC B cells (Fig. 3A–D). This result suggests that TLR7 is absolutely required for Spt-GC formation in B6.*Sle1b* mice. In contrast, *Sle1b*/TLR9-KO mice had a 2-fold higher percentage of Spt-GC B cells than did B6.*Sle1b* controls (Fig. 3A, 3C) and also had increased Tfh cells (Fig. 3B, 3D). Immunofluorescence analysis yielded similar results. $IgD^{-}GL7^{+}$ Spt-GC B cells could not be detected in *Sle1b*/TLR7-KO mice, whereas *Sle1b*/TLR9-KO mice had more of these cells than did B6.*Sle1b* controls (Fig. 3E). In accordance with the GC profiles, the numbers of IgM^{+} AFCs or IgG^{+} AFCs were near background levels in *Sle1b*/TLR7-KO mice, but they were significantly higher in *Sle1b*/TLR9-KO mice than in the B6.*Sle1b* controls (Fig. 3F, 3G). Additionally, the total IgG serum titers were significantly lower in *Sle1b*/TLR7-KO mice compared with B6.*Sle1b* mice. The difference was more pronounced in the titers of the IgG2b and IgG2c subclasses. However, the loss of TLR9 did not significantly affect any of the serum Ab titers in the B6.*Sle1b* mice (Fig. 3H).

Consistent with previous reports (10, 11), both *Sle1b*/TLR9-KO and *Sle1b*/TLR7-KO mice had significantly fewer anti-DNA, anti-histone, and anti-nucleosome AFCs than did B6.*Sle1b* mice, with the lowest values observed in *Sle1b*/TLR7-KO mice (Fig. 4A). We used a fluorescent ANA assay to directly measure RNA- and DNA-specific autoantibodies. Serum from B6.*Sle1b* mice showed a bright and uniform nuclear staining pattern. Very faint nuclear staining was observed with serum from *Sle1b*/TLR7-KO mice, whereas a uniform, but faint, cytoplasmic staining was observed with serum from *Sle1b*/TLR9-KO mice (Fig. 4B). Measurement of the amount of anti-Sm/RNP IgG subclasses in the sera showed significant decreases in IgG1 and IgG2c in *Sle1b*/TLR7-KO mice, whereas *Sle1b*/TLR9-KO mice had levels comparable to B6.*Sle1b* mice (Fig. 4C). A marked decrease in all subclasses of anti-cardiolipin Abs was observed in *Sle1b*/TLR7-KO mice. However, a significant decrease was only noted in anti-cardiolipin IgG2c subclass in *Sle1b*/TLR9-KO mice compared with *Sle1b* mice (Fig. 4D).

These data indicate that, in the absence of TLR7-mediated Spt-GC B cell and Tfh cell responses, the production of autoantibodies against RNA-associated self-Ags (Sm/RNP), as well as with specificities for nuclear Ags (dsDNA, histone and nucleosome) and nonnuclear Ags (cardiolipin), is markedly compromised. These results emphasize the importance of the GC pathway and TLR7 in generating autoantibodies with diverse specificities.

Although B6.*Sle1b* mice develop high titers of ANAs (29), they do not show severe lupus nephritis and associated mortality (36). However, B6.*Sle1b* mice in combination with the *yaa* locus develop highly penetrant glomerulonephritis (51). Similarly, TLR7 activation by imiquimod (IMQ) also induces glomerulonephritis in MRL/*lpr* mice (19). Conversely, loss of TLR7 in MRL/*lpr* mice ameliorates kidney disease (11). To address the contribution of TLR signaling in kidney pathology of B6.*Sle1b* mice, we evaluated the glomerular immune complex and complement deposition by immunofluorescence staining. Consistent with the reported literature and the serum autoantibody titers, total IgG and C3 deposition in the kidney sections of B6.*Sle1b*/TLR7-KO mice was significantly reduced (Supplemental Fig. 2). However, as opposed to other lupus-prone mouse models (11, 20), TLR9 deficiency in B6.*Sle1b* mice did not exacerbate glomerular IgG and C3 deposition compared with B6.*Sle1b* mice (Supplemental Fig. 2). Instead, in conjunction with the reduced serum levels of ANAs, we observed reduced glomerular IgG deposition (Supplemental Fig. 2).

*Autoantibody production strongly correlates with elevated Spt-GC B cell and Tfh cell responses in B6.*Sle1b.yaa *mice*

A recent report by Hwang et al. (31) showed increased Tfh cell and autoantibody responses, but reduced MZ B cells, in B6.*Sle1.yaa* mice (expressing the *Sle1* interval and *yaa* locus bearing two copies of TLR7). The effect of epistatic interaction between the *Sle1* and *yaa* loci on Spt-GCs was not examined in these mice. *Sle1* is a long interval consisting of four subloci: *Sle1a*, *Sle1FcR*, *Sle1b*, and *Sle1c*. B6 mice congenic for each sublocus display varying autoimmune phenotypes (36), and the epistatic interaction of each sublocus with the *yaa* locus may have differential outcomes. Given our data that TLR7 deficiency eliminated Spt-GCs, we asked whether an extra copy of TLR7 could enhance the Spt-GC B cell and Tfh cell responses in B6.*Sle1b* mice. We crossed B6.*Sle1b* mice with the B6.*yaa* strain to generate B6.*Sle1b.yaa* mice. The percentages of GC B cells and Tfh cells were strikingly higher in B6.*Sle1b.yaa* males compared with B6, B6.*yaa*, and B6.*Sle1b* males (Fig. 5A, 5B). These data indicate that the epistatic interaction of *Sle1b* and *yaa* affects the GC-tolerance pathway of autoantibody production.

In addition to TLR7, the translocated *Yaa* locus from the X chromosome contains 15 other genes (52). To ascertain whether in vivo TLR7 stimulation with an agonist alone could enhance the Spt-GC responses, we treated age- and sex-matched naive B6 and B6.*Sle1b* mice with the TLR7 agonist IMQ. There was no significant difference observed in the percentages of Spt-GC B cells and Tfh cells between IMQ- and PBS-treated B6 mice (Fig. 5C, 5D). However, B6.*Sle1b* mice treated with IMQ had significantly increased percentages of GC B cells and Tfh cells compared with PBS-treated controls (Fig. 5C, 5D).

Across the full array of responses, B6.*Sle1b.yaa* mice showed levels that were significantly higher than in B6, B6.*yaa*, or B6.*Sle1b* mice. These responses included the production of AFCs against DNA, histone, and nucleosome (Fig. 5E–G); elevated levels of pathogenic IgG2b and IgG2c autoantibodies against DNA, histone, and nucleosome (Fig. 5H–J); and IgM, IgG2b, and IgG2c Abs against Sm/RNP (Fig. 5K) or cardiolipin (Fig. 5L). These data indicate that the expression of an extra copy of TLR7 in the *Sle1b* genetic background and the resulting increase in Spt-GC B cell and Tfh cell responses was sufficient to enhance a broad autoimmune signature.

B cell–intrinsic TLR7 expression controls steady-state Spt-GC formation and Tfh cell development

To determine the B cell–specific function of TLR7 in the formation of Spt-GC B cells and Tfh cells, we chose the non-autoimmune B6 mouse model in which we could eliminate the contribution of autoimmune-susceptibility genes and the overexpression of TLR7. We generated mixed BM chimeras by reconstituting lethally irradiated B6.μMT mice, which lack mature B cells, with a mixture of BM cells. Eighty percent of the transferred BM cells were derived from μMT mice, and 20% were

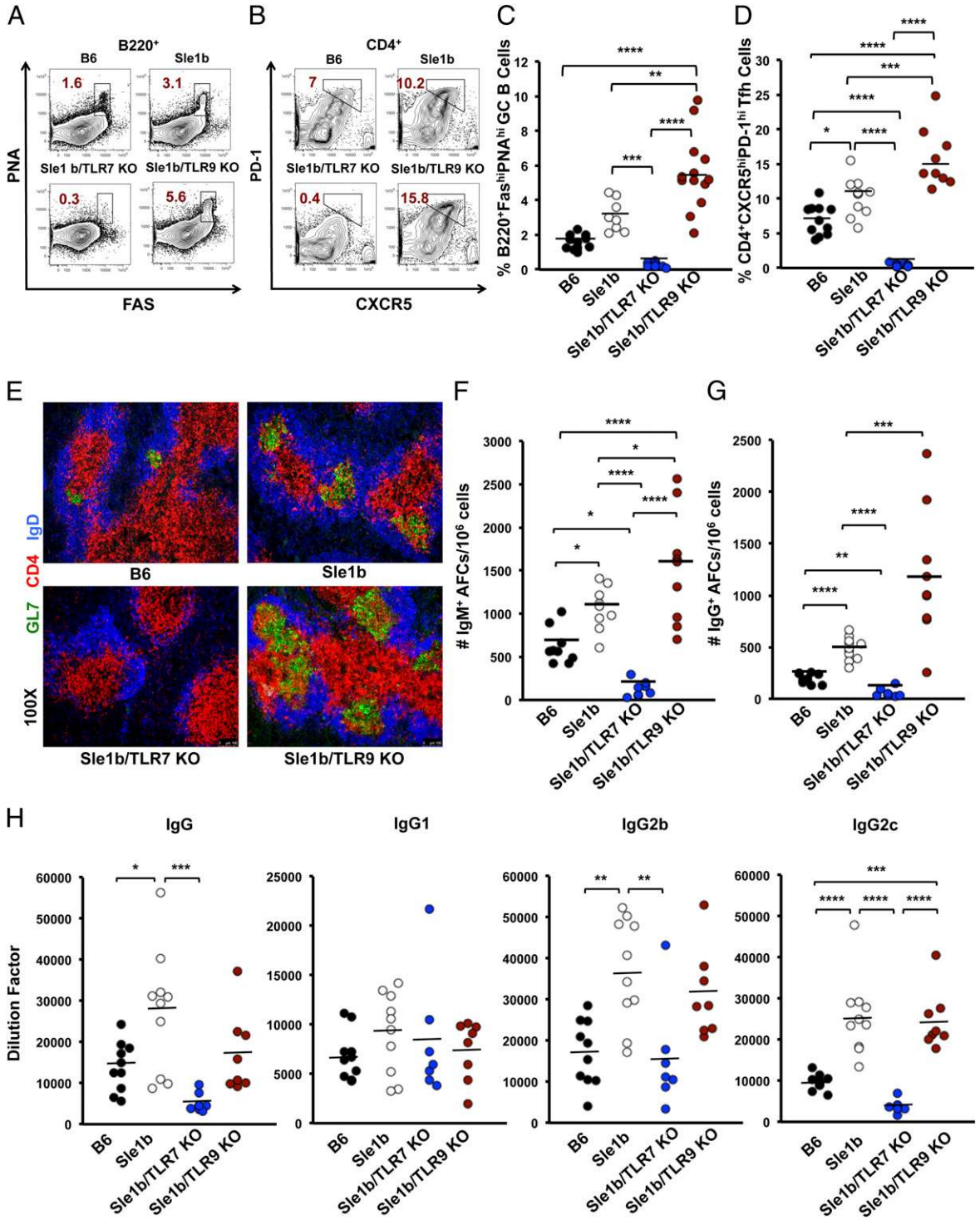

FIGURE 3. Spt-GCs fail to develop in B6.*Sle1b* mice in the absence of TLR7. Representative contour plots show the gating strategy for GC B cells (**A**) and Tfh cells (**B**). Scatter plots show the percentage of GC B cells (**C**) and Tfh cells (**D**). (**E**) Representative spleen sections from 6-mo-old mice stained with GL-7 (green), anti-CD4 (red), and anti-IgD (blue). Data are representative of at least three or four mice analyzed per group. Original magnification ×100. ELISPOT analysis of IgM^+ (**F**) and IgG^+ (**G**) AFCs at 6 mo of age. (**H**) Total anti-IgG–specific, anti-IgG1–specific, anti-IgG2b–specific, and anti-IgG2c–specific serum Ab titers in the indicated mice at 6 mo of age. Each circle represents an individual female mouse. *$p \leq 0.05$, **$p \leq 0.01$, ***$p \leq 0.001$, ****$p \leq 0.0001$.

derived from B6, TLR9-KO, or TLR7-KO mice. The mice were rested for 3 mo and then analyzed. We found the complete absence of IgD^-GL7^+ Spt-GC B cells in μMT mice that received BM cells from TLR7-KO mice, whereas the chimeras that received B6 or TLR9-KO BM cells developed the typical staining pattern of Spt-GCs (Fig. 6A). Quantification by flow cytometry supported the imaging results (Fig. 6B, 6C). We confirmed our results by adoptively transferring B cells from B6, TLR7-KO, or TLR9-KO mice along with T cells from B6 mice into Rag1-KO mice. Consistent with the BM chimeras, Rag1-KO mice that received TLR7-KO B cells did not develop any Spt-GCs, whereas well-formed GCs were observed in mice receiving B6 or TLR9-KO B cells (Fig. 6D). Similar results were obtained by flow cytometry analysis of GC B cells (Fig. 6E, 6F). Additionally, Rag1-KO mice

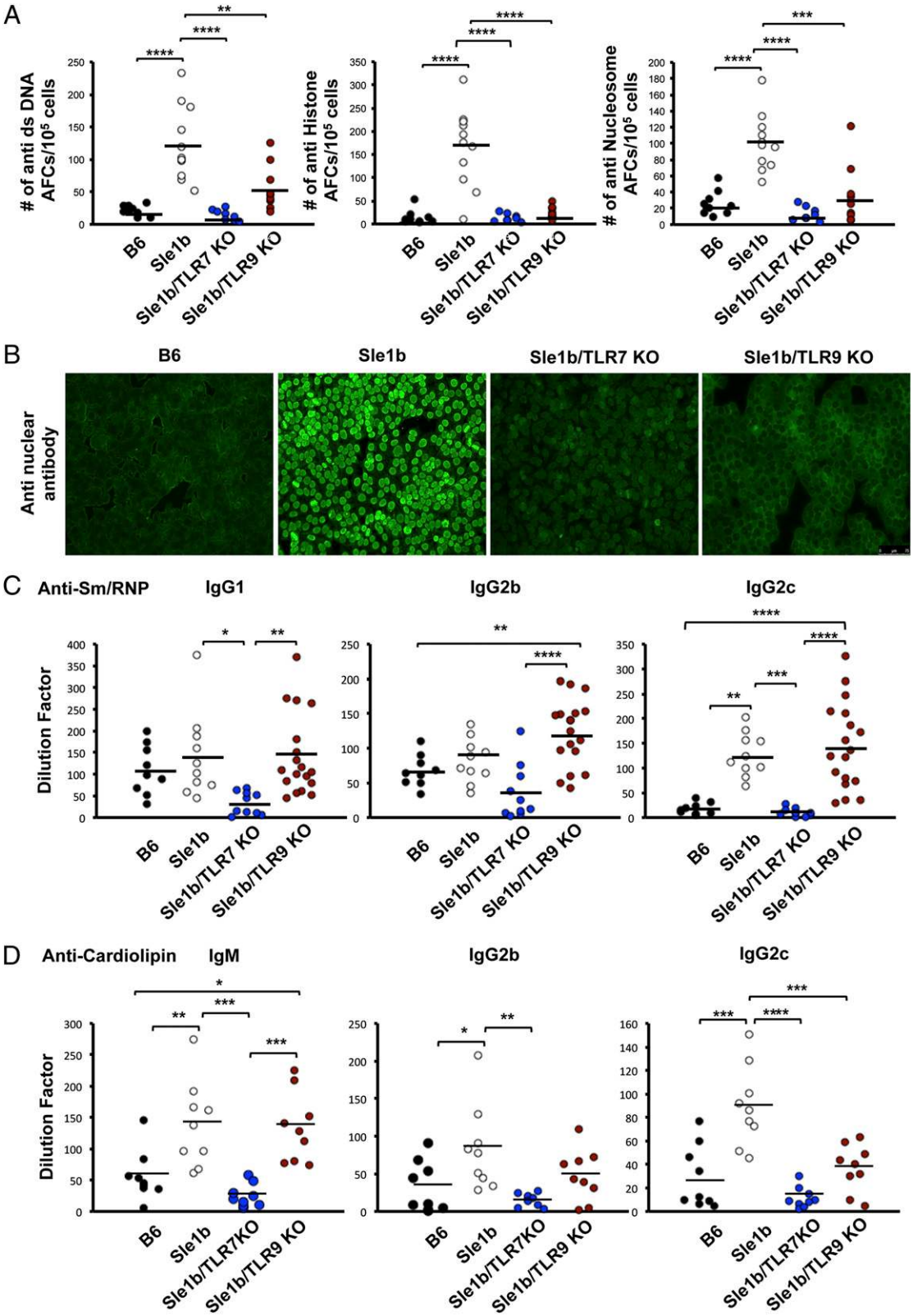

FIGURE 4. TLR7 and TLR9 regulate autoantibody titers in B6.*Sle1b* mice. (**A**) ELISPOT analysis shows anti-dsDNA–specific, anti-histone–specific, and anti-nucleosome–specific AFCs in splenocytes of the indicated mice. (**B**) ANA detection using Hep-2 culture slides stained with serum (1:50 dilution in PBS) from the indicated mouse strains. Data are representative of at least 8–10 serum samples analyzed per mouse strain. (**C**) Anti-Sm/RNP–specific IgG1, anti-Sm/RNP–specific IgG2b, and anti-Sm/RNP–specific IgG2c serum Ab titers in the indicated mice. (**D**) Anti-cardiolipin–specific IgM, anti-cardiolipin–specific IgG2b, and anti-cardiolipin–specific IgG2c serum Ab titers in the indicated mice. Each circle represents an individual female mouse. $*p \leq 0.05$, $**p \leq 0.01$, $***p \leq 0.001$, $****p \leq 0.0001$.

receiving TLR7-KO B cells had significantly fewer IgM^+ AFCs and IgG^+ AFCs than did mice populated with B6 or TLR9-KO B cells (Fig. 6G, 6H).

We also examined whether myeloid cell–intrinsic TLR-MyD88 signaling is directly involved in controlling steady-state Spt-GC formation in nonautoimmune B6 mice. Three-month-old $MyD88^{fl/fl}$,

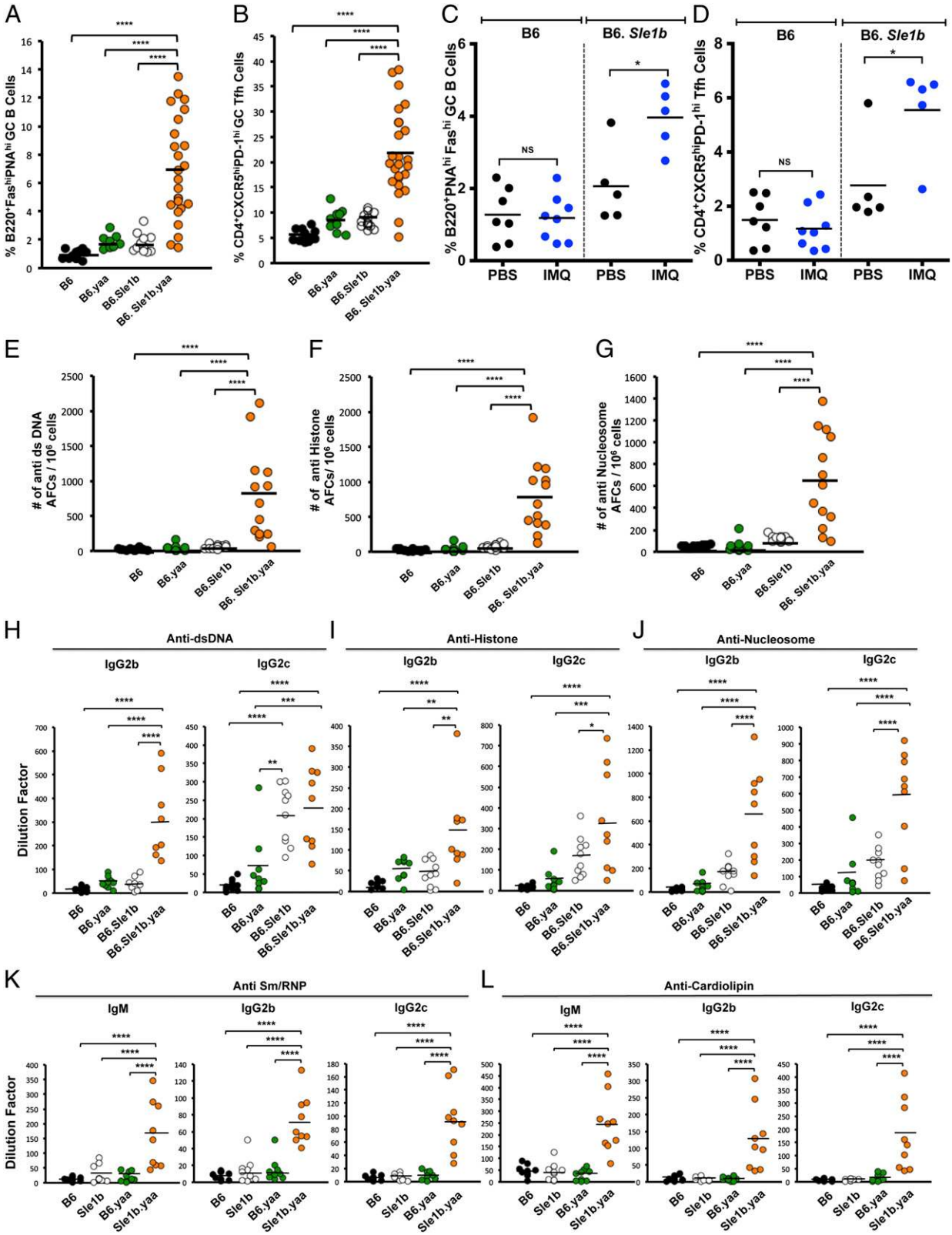

FIGURE 5. Increased TLR7 expression enhances Spt-GCs and autoantibody production in B6.*Sle1b.yaa* mice. Scatter plots show percentages of GC B cells (**A**) and Tfh cells (**B**) in the indicated strains. (**C** and **D**) Two-month-old mice from the indicated strains were injected i.p. with 200 μl PBS or with 25 μg IMQ in 200 μl PBS twice a week for 6 wk. Scatter plots show the percentage of GC B cells (C) and Tfh cells (D) in B6 and B6.*Sle1b* mice treated with PBS or IMQ. ELISPOT analysis of anti-dsDNA (**E**), anti-histone (**F**), and anti-nucleosome (**G**) AFCs in total splenocytes of the indicated mice. Serum titers of IgG2b and IgG2c subclass Abs specific for dsDNA (**H**), histone (**I**), and nucleosome (**J**). (**K**) Anti-Sm/RNP–specific IgM, anti-Sm/RNP–specific IgG2b, and anti-Sm/RNP–specific IgG2c serum Ab titers. (**L**) Anti-cardiolipin–specific IgM, anti-cardiolipin–specific IgG2b, and anti-cardiolipin–specific IgG2c serum Ab titers measured by ELISA from the indicated mice. Each circle represents an individual mouse. $*p \leq 0.05$, $**p \leq 0.01$, $***p \leq 0.001$, $****p \leq 0.0001$.

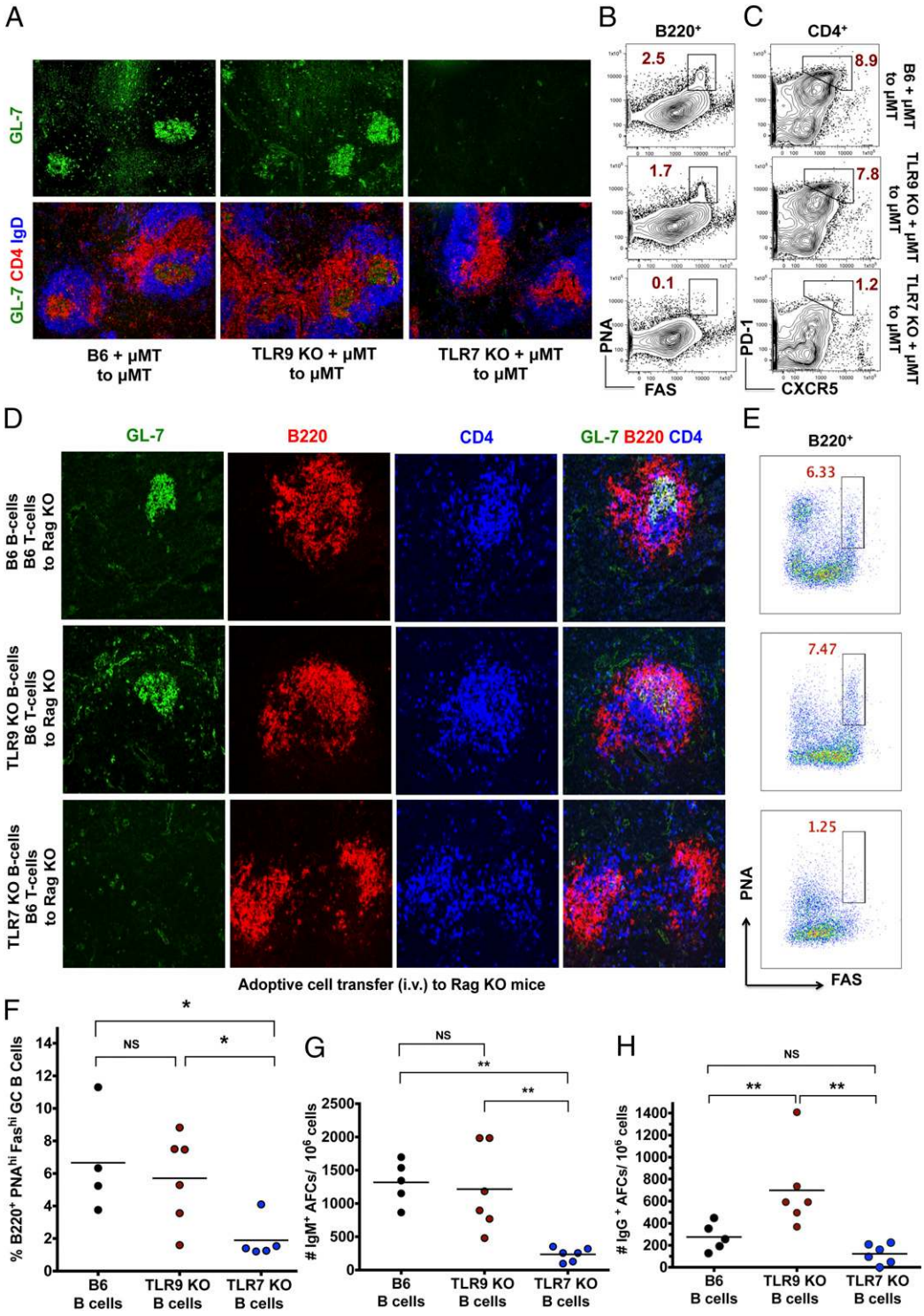

FIGURE 6. B cell–intrinsic TLR7 signaling is required for Spt-GC formation. Mixed BM chimeric mice were generated as described in *Materials and Methods*. (**A**) Representative spleen sections of the indicated chimeras stained with GL-7 (green), anti-CD4 (red), and anti-IgD (blue). Original magnification ×100. Representative contour plots show GC B cells (**B**) and Tfh cells (**C**) from the indicated chimeras. (**D**) B and T cells were adoptively transferred into Rag1-KO mice, as described in *Materials and Methods*. Spleen sections of Rag1-KO mice were stained as in (A). Original magnification ×100. (**E**) Representative dot plots show gating strategy for GC B cells (in rectangles) in Rag1-KO mice transferred with B cells from B6 (*upper panel*), TLR9-KO (*middle panel*), or TLR7-KO (*lower panel*) mice. (**F**) Scatter plots show the percentage of GC B cells in Rag1-KO mice transferred with B cells from the indicated strains. ELISPOT analysis of IgM^+ (**G**) and IgG^+ (**H**) AFCs in splenocytes of Rag1-KO mice transferred with B6, TLR9-KO, or TLR7-KO B cells. Four or five mice were analyzed per genotype for the immunofluorescence analysis. Each circle represents an individual mouse. $*p \leq 0.05$, $**p \leq 0.01$.

LySM-$Cre^{+/-}$-$MyD88^{fl/fl}$, and CD11c-$Cre^{+/-}$-$MyD88^{fl/fl}$ mice had similar Spt-GC B cell and Tfh cell profiles (Fig. 7), arguing against a myeloid cell–intrinsic TLR7-MyD88 signaling requirement for the development of steady-state Spt-GCs. These data strongly suggest that the expression of at least one copy of TLR7 specifically in B cells is necessary for Spt-GC B cell and Tfh cell formation.

Suboptimal B cell proliferation and survival in the absence of TLR7 signaling

Next, we evaluated whether the absence of Spt-GCs in TLR7-KO mice resulted from a defect in B cell proliferation and survival. *Sle1b*/TLR9-KO mice had significantly higher $IgD^{-}Ki67^{+}$ proliferating GC B cells than did B6 or B6.*Sle1b* controls, but B cell follicles of *Sle1b*/TLR7-KO spleens completely lacked $Ki67^{+}$ cells (Fig. 8A). The deficiency in TLR7 did not affect the number of $Ki67^{+}$ cells outside the follicles (Fig. 8A). We also performed an ex vivo proliferation assay in which B cells were stimulated with anti-IgM and anti-CD40 (without any exogenous TLR ligands). As gauged by the CFSE dilution, a significantly reduced percentage of B cells deficient in TLR7 or MyD88 underwent cell divisions compared with B6 and TLR9-KO B cells (Fig. 8B, 8C). Moreover, naive TLR7-KO B cells cultured or not with stimulation secreted reduced titers of IgG in the culture supernatant compared with TLR9-KO and B6 B cells (Fig. 8D, 8E).

To investigate whether this proliferative defect also occurred in vivo, we transferred CFSE-labeled naive B cells from B6, TLR7-KO, or TLR9-KO mice into B6.μMT mice preimmunized with SRBCs. Once again, TLR7-KO B cells proliferated to a lesser extent than did TLR9-KO or B6 B cells (Fig. 8F, 8G). The results described above prompted us to evaluate whether B cell survival was compromised upon BCR stimulation. We found a 2-fold reduction in the percentage of live TLR7-KO B cells compared with B6 and TLR9-KO B cells after >48 h of stimulation with anti-IgM and anti-CD40 (Fig. 9A).

Cell cycle analysis by PI staining of B cells, cultured for 72 h after stimulation with anti-IgM and anti-CD40, showed a significantly higher percentage of TLR7-KO B cells in the apoptotic sub-G_1 population, but a lower percentage in the G_0-G_1 and S-G_2/M phase, compared with B6 B cells (Fig. 9B). The addition of BAFF to in vitro B cell–proliferation cultures was unable to rescue TLR7-KO B cells from cell death (Fig. 9C, 9D). These ex vivo data indicate that B cell proliferation and survival are suboptimal in the absence of TLR7 signaling via MyD88. Taken together, our results suggest that B cell–specific TLR7-MyD88 signaling and B cell survival/proliferation are necessary for Spt-GC formation and Ab production.

We also compared the transcript levels of key factors involved in GC formation and maintenance. Consistent with elevated Spt-GC, Tfh cell, and AFC responses, splenocytes from TLR9-KO and B6.*yaa* mice expressed higher levels of PD-1, ICOS, and Xbp-1 transcripts than did B6 and TLR7-KO mice (Supplemental Fig. 3A–C). B6.*yaa* splenocytes expressed more Bcl-6 mRNA than did B6, TLR9-KO, or TLR7-KO splenocytes (Supplemental Fig. 3E), but the IRF-4 transcript level was comparable among all groups (Supplemental Fig. 3D). We found that *Aicda* mRNA levels were directly proportional to the dose of TLR7 and inversely proportional to the dose of TLR9. Therefore, *Aicda* mRNA expression in purified B cells fell into the following hierarchy: B6.yaa > TLR9-KO > B6 > TLR7-KO (Supplemental Fig. 3F).

Discussion

Spt-GC B cells and Tfh cells play a significant role in generating high-affinity pathogenic autoantibodies in murine models of lupus and human SLE (53). Previous studies elucidated the role of TLRs in B cell activation, autoantibody specificity, and lupus pathogenesis. However, the mechanisms underlying TLR-dependent differential regulation of Spt-GC B cell and Tfh cell formation are not clear. In nonautoimmune mice, the involvement of MyD88, TLR7, and TLR9 in the enhancement of B cell Ab production has been discussed extensively in the context of active immunizations. The antigenic sources include various T-dependent Ags (mixed with or conjugated to TLR ligands), RNA/DNA viruses, virus-like particles, or bacterial infections (inherently carrying natural TLR ligands) (54–58). However, the involvement of TLR signaling under steady-state conditions, with an antigenic repertoire comprising self-Ags derived from apoptotic cells (59, 60) or endogenous microbial agents, has not been discussed.

Our analysis of various TLR-deficient B6 mice revealed that GCs that are spontaneously formed in the absence of exogenous stimuli are entirely dependent on TLR7 signaling via MyD88.

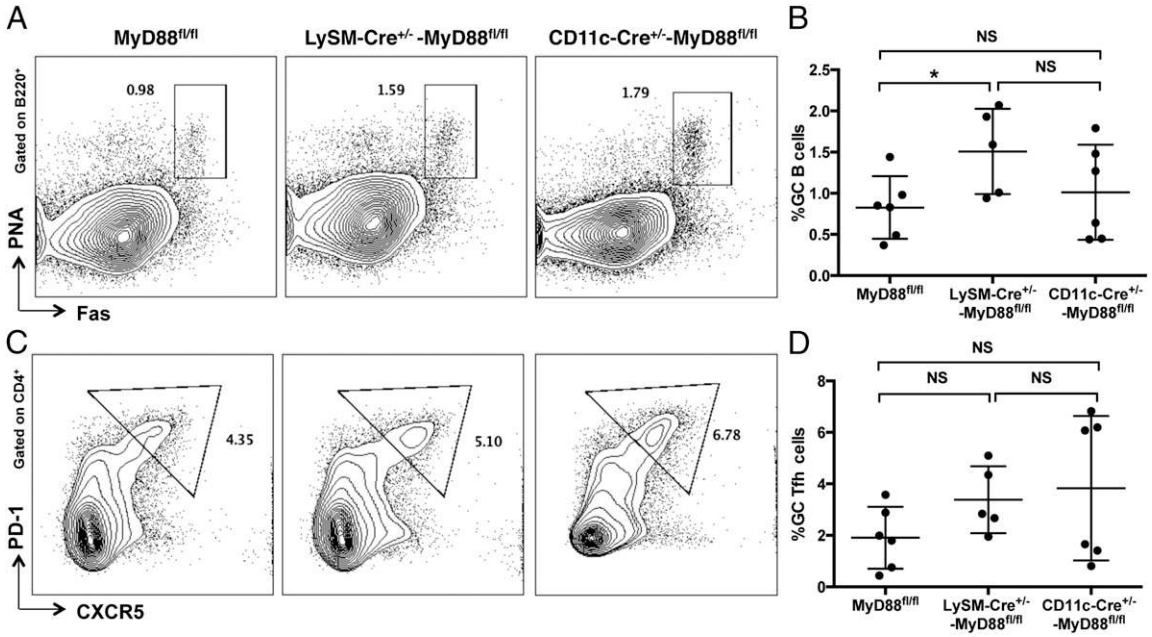

FIGURE 7. MyD88 deficiency in macrophages and DCs does not affect Spt-GC formation. Representative contour plots show the gating strategy (**A**) and scatter plots show the percentage of GC B cells (**B**) in the indicated mouse strains. Representative contour plots show the gating strategy (**C**) and scatter plots show the percentage of Tfh cells (**D**) in the indicated mouse strains. Each circle represents an individual mouse.

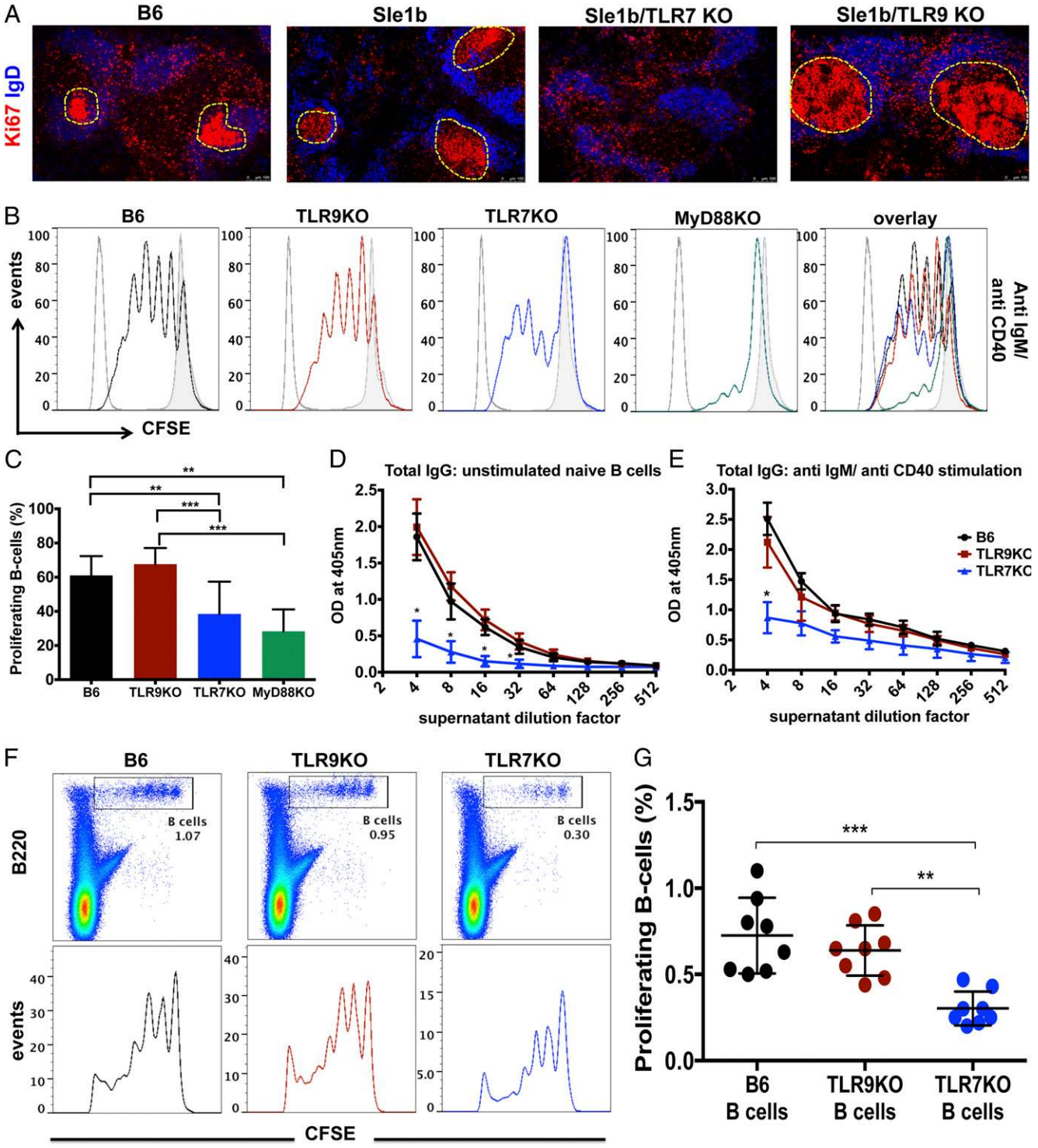

FIGURE 8. TLR7-MyD88 signaling is required for optimal B cell proliferation. (**A**) Representative immunofluorescence analysis of spleen sections from three or four 6-mo-old mice stained for Ki67 (red) and IgD (blue). GCs are outlined. Original magnification ×100. (**B**) Representative graphs show the proliferation profile of CFSE-labeled B cells from the indicated mice stimulated with anti-IgM/anti-CD40 for 72 h. Solid gray lines represent CFSE-labeled unstimulated cells, and dashed gray lines represent unlabeled unstimulated B cells. (**C**) Bar graph shows the percentage of in vitro proliferating B cells in the indicated mouse strains stimulated with anti-IgM/anti-CD40 for 72 h and assessed by flow cytometry. Error bars represent ±SEM. Analysis of total IgG secreted in culture supernatants of unstimulated B cells (**D**) or B cells stimulated with anti-IgM/anti-CD40 for 72 h (**E**), as assessed by ELISA. Error bars represent ±SD. In vitro data are representative of four independent experiments with three or four sex-matched 8–10-wk-old mice/group. (**F**) Pseudocolor plots show the gating of in vivo–proliferating B cells (labeled with CFSE) from the indicated strains, which were transferred into μMT mice preimmunized with SRBCs (*upper panels*). Profiles of in vivo–proliferating transferred B cells, as assessed by decreasing CFSE fluorescence intensity (*lower panels*). (**G**) Percentage of in vivo–proliferating B cells [as described for (F)] from the indicated strains. Error bars represent ±SD. Each circle represents an individual mouse. $*p \leq 0.05$, $**p \leq 0.01$, $***p \leq 0.001$.

Unlike B6 mice, TLR7-KO mice did not develop Spt-GCs, even by the age of 6 mo. In contrast, TLR9-KO mice had increased numbers of Spt-GCs. However, upon immunization with T-dependent Ags, TLR7-KO mice developed GC B cells and Tfh cells, although to a significantly lesser extent than did B6 mice (Supplemental Fig. 4). Again, in the absence of TLR9, the GC responses to these

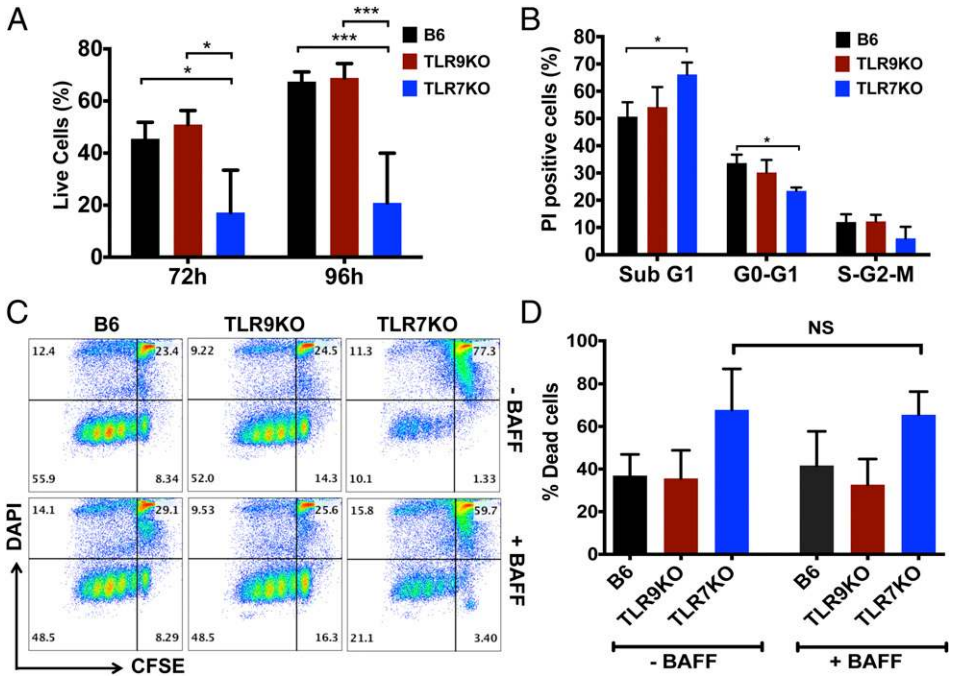

FIGURE 9. TLR7 deficiency leads to compromised B cell survival. (**A**) Percentage of live cells assessed by DAPI staining of purified B cells that were stimulated with anti-IgM and anti-CD40 for 72 or 96 h from the indicated mouse strains. (**B**) Cell cycle analysis of purified B cells from the indicated strains at 72 h after stimulation with anti-IgM and anti-CD40. (**C**) Pseudocolor dot plots represent the percentage of live and dead CFSE-labeled B cells, as assessed by DAPI staining, from the indicated strains that were stimulated in vitro with anti-IgM and anti-CD40, with or without BAFF, for 72 h. (**D**) Percentage of $DAPI^+$ cells from three independent experiments in (C). Error bars represent ±SEM. Data are representative of four independent experiments with three or four sex-matched 8–10-wk-old mice/group. $*p \leq 0.05$, $***p \leq 0.001$.

exogenous Ags were elevated (Supplemental Fig. 4). These studies highlight the important stimulatory role of TLR7-MyD88 signaling in the GC pathway. Our data also identify TLR9 as a repressor of TLR7 activity during a GC reaction under non-autoimmune conditions.

B cell differentiation and autoantibody production primarily proceed through the extrafollicular and FO GC pathways. MRL/*lpr* mice have been used extensively to study the role of TLR7 and TLR9 in murine lupus, including the specificity of anti-nuclear Abs and kidney pathology (15). The autoreactive B cells in MRL/*lpr* mice proliferate and undergo somatic hypermutation outside the follicles in the T cell zone (30). Studies in the AM14 and MRL/*lpr* dual model systems suggested that both T-dependent and T-independent mechanisms are responsible for TLR7- or TLR9-mediated extrafollicular activation, expansion, and differentiation of the AM14 rheumatoid factor B cells (61). Similarly, in TLR7.1Tg mice, splenic red pulp is the primary site for the activation and proliferation of anti-RNA–specific transitional type 1 B cells in the periphery (46). Additionally, in lupus-prone BAFF-Tg mice, autoantibody production involves MyD88-TLR–dependent expansion of autoreactive MZ and B1 B cells but not GC B cells (62). Together, these studies highlight the importance of TLR7 or TLR9 in regulating spontaneously activated B cells in the extrafollicular regions but not in the FO GC pathway of B cell differentiation.

Many autoimmune mouse models, including (NZB/NZW) F1, BXSB.*yaa*, and sanroque, spontaneously develop increased GC B cells, Tfh cells, and high titers of serum autoantibodies (22, 52, 63, 64). Recently, Hua et al. (33) showed the requirement of GCs and MyD88-signaling in ANA production and nephritis in Lyn-deficient mice. These autoimmune mouse models highlight the significance of the FO GC pathway in B cell responses and autoantibody production but do not delineate the contribution or requirement for TLR7 and TLR9 in Spt-GC formation. A recent publication by Rawlings and colleagues (20) focused on the roles of TLR7 and TLR9 signaling in immune cell activation, autoantibody repertoire, systemic inflammation, and kidney pathology using the WASp autoimmune mouse model. Although this study addresses the opposing effects of B cell–intrinsic TLR7 and TLR9 expression on immune activation, including GC B cells and Tfh cells, it does not define the mechanisms by which TLRs control the formation of Spt-GC B cells and Tfh cells.

Consistent with our observations in B6 mice and the results reported using the WASp model (20), we found that TLR7 is absolutely essential for Spt-GC formation in B6.*Sle1b* mice, whereas TLR9 signaling inhibited such responses. Supplementation of an extra copy of TLR7 (*yaa* locus) in B6.*Sle1b* mice or treatment of B6.*Sle1b* mice with a TLR7 agonist increased the Spt-GC B cell, Tfh cell, and autoantibody responses. These data indicate that Spt-GCs can help to breach B cell tolerance at the GC checkpoint either in the presence of genetic predisposition along with one copy of TLR7 or when TLR7 alone is overexpressed. The role of TLR7 in promoting Spt-GC and Tfh cell responses was examined previously using two mouse models: one expressed 15–18 copies of TLR7 on a B6 background (32), and the other expressed two or three copies of TLR7 on the *Sle1* background (31). B cell–intrinsic expression of 15–18 copies of TLR7 promoted Spt-GC and plasmablast development, whereas a 2-3–fold increase in B cell TLR7 expression resulted in enhanced splenic B and T cell activation, MZ B cell reduction but did not promote Spt-GC, Tfh cell, and plasmablast development. These two models allowed for the investigation of the role of TLR7 overexpression in the enhancement of B and T cell responses; however, these studies did not determine whether TLR7 is required for the initiation of Spt-GCs. Our study directly addresses the function of a single copy of the TLR7 gene in the initiation of Spt-GCs under nonautoimmune and autoimmune conditions.

Our results also show that TLR7 has a major role in promoting the generation of autoantibodies through the formation of Spt-GCs and that TLR9 inhibits the TLR7-mediated FO GC responses in B6.*Sle1b* mice. This model addresses the potential epistatic interaction between TLRs and the lupus-associated SLAM family genes in breaking the GC tolerance checkpoint. Recent studies showed that the deficiency in nucleic acid–sensing TLR signaling due to mutations in Unc93b1 is sufficient to interfere with the generation of ANAs (65, 66). Additionally, other pathogenic nonnuclear autoantibody specificities, including anti-cardiolipin, anti-RBC, and

anti-myeloperoxidase, which are commonly found in SLE patients, also are reduced by Unc93b1 mutations (65, 66). Our work extends those observation and defines TLR7 as the key nucleic acid–sensing TLR for the production of nuclear and nonnuclear Ag-specific autoantibodies.

B6 mice deficient in both TLR8 and TLR9 were reported to develop a stronger autoimmune response than either TLR8-KO or TLR9-KO mice, implying that TLR8 and TLR9 can independently suppress TLR7-mediated autoimmunity (67). However, another study using 564Igi mice with knock-in genes encoding an autoreactive anti-RNA Ab showed that, upon single deletions of TLR7, TLR8, or TLR9 or combined deletion of TLR7 and TLR9, autoantibodies were still produced but removing TLR7 and TLR8 together abolished the autoantibody production (68). These conflicting results about the role of TLR8 have yet to be explained.

Our adoptive-transfer and BM chimera studies demonstrated that TLR7 signaling in B cells is essential for the formation of Spt-GC B cells and Tfh cells in B6 mice. Other investigators (40) proposed that TLR-stimulated dendritic cells (DCs) can induce a strong Ag-dependent Th cell response, which, in turn, can promote extrafollicular and GC-mediated Ab responses. TLR7 signaling also is implicated in the activation of plasmacytoid DCs (11). However, we did not observe any direct effect of TLR7 signaling in DCs on the formation of steady-state Spt-GCs and Tfh cells.

TLR7 overexpression was shown to promote the proliferation of transitional type 1 B cells (46). Also, TLR7 signaling was shown to be important for GC B cell proliferation during chronic viral infection (57). However, the effect of TLR7 and MyD88 signaling on B cell proliferation in the absence of TLR7 overexpression or infection is not clear. We found significantly reduced proliferation of B cells in TLR7-KO and MyD88-KO mice compared with B6 controls. Moreover, the total percentage of dead B cells after 48 h of activation was significantly higher in TLR7-KO mice compared with B6 and TLR9-KO mice. TLR-MyD88 signaling induces the expression of genes that control cell survival and proliferation (69–71); hence, it is very likely that the prosurvival and/or proliferative signals transduced by TLR7-MyD88 signaling are critical specifically within the Spt-GC microenvironment where B cell antigenic stimulation is not overwhelming. It is conceivable that during the formation of Spt-GCs, caused by mild B cell antigenic stimulation, the TLR7-MyD88–induced signals become equally necessary for the sustenance of B cells within GCs. The cause of the disparity in outcomes between the signals transduced by TLR7 and TLR9, which are thought to use the same signaling intermediates, remains to be determined.

Our finding that TLR7 signaling is required for the optimal survival of B cells, thereby promoting GC formation and Ab/autoantibody production predominantly through the FO GC pathway, has therapeutic implications for the treatment of SLE and other humoral immune response–mediated autoimmune disorders. Modulating the FO GC pathway by targeting TLR7 signaling in B cells may be an effective strategy to decrease autoantibody production against diverse autoantigens.

Acknowledgments

We thank Drs. Aron Lukacher, David Spector, and Todd Schell for critical reading of the manuscript and helpful discussions. We thank Dr. Daniel Mucida for providing spleens from germ-free mice and Dr. Milena Bogunovic for helpful discussions and providing spleens from MyD88$^{fl/fl}$, CD11c-Cre$^{+/-}$-MyD88$^{fl/fl}$, and LysM-Cre$^{+/-}$-MyD88$^{fl/fl}$ mice. We also thank Stephanie Schell for proofreading the manuscript. Finally, we thank Melinda Elias for technical assistance, as well as the Pennsylvania State University College of Medicine Flow Cytometry Core Facility.

Disclosures

The authors have no financial conflicts of interest.

References

1. Inamine, A., Y. Takahashi, N. Baba, K. Miyake, T. Tokuhisa, T. Takemori, and R. Abe. 2005. Two waves of memory B-cell generation in the primary immune response. *Int. Immunol.* 17: 581–589.
2. MacLennan, I. C. 1994. Germinal centers. *Annu. Rev. Immunol.* 12: 117–139.
3. Jacob, J., G. Kelsoe, K. Rajewsky, and U. Weiss. 1991. Intraclonal generation of antibody mutants in germinal centres. *Nature* 354: 389–392.
4. Berek, C., A. Berger, and M. Apel. 1991. Maturation of the immune response in germinal centers. *Cell* 67: 1121–1129.
5. Blink, E. J., A. Light, A. Kallies, S. L. Nutt, P. D. Hodgkin, and D. M. Tarlinton. 2005. Early appearance of germinal center-derived memory B cells and plasma cells in blood after primary immunization. *J. Exp. Med.* 201: 545–554.
6. Benner, R., W. Hijmans, and J. J. Haaijman. 1981. The bone marrow: the major source of serum immunoglobulins, but still a neglected site of antibody formation. *Clin. Exp. Immunol.* 46: 1–8.
7. Takahashi, Y., P. R. Dutta, D. M. Cerasoli, and G. Kelsoe. 1998. In situ studies of the primary immune response to (4-hydroxy-3-nitrophenyl)acetyl. V. Affinity maturation develops in two stages of clonal selection. *J. Exp. Med.* 187: 885–895.
8. Genestier, L., M. Taillardet, P. Mondiere, H. Gheit, C. Bella, and T. Defrance. 2007. TLR agonists selectively promote terminal plasma cell differentiation of B cell subsets specialized in thymus-independent responses. *J. Immunol.* 178: 7779–7786.
9. Rubtsov, A. V., C. L. Swanson, S. Troy, P. Strauch, R. Pelanda, and R. M. Torres. 2008. TLR agonists promote marginal zone B cell activation and facilitate T-dependent IgM responses. *J. Immunol.* 180: 3882–3888.
10. Christensen, S. R., M. Kashgarian, L. Alexopoulou, R. A. Flavell, S. Akira, and M. J. Shlomchik. 2005. Toll-like receptor 9 controls anti-DNA autoantibody production in murine lupus. *J. Exp. Med.* 202: 321–331.
11. Christensen, S. R., J. Shupe, K. Nickerson, M. Kashgarian, R. A. Flavell, and M. J. Shlomchik. 2006. Toll-like receptor 7 and TLR9 dictate autoantibody specificity and have opposing inflammatory and regulatory roles in a murine model of lupus. *Immunity* 25: 417–428.
12. Ehlers, M., H. Fukuyama, T. L. McGaha, A. Aderem, and J. V. Ravetch. 2006. TLR9/MyD88 signaling is required for class switching to pathogenic IgG2a and 2b autoantibodies in SLE. *J. Exp. Med.* 203: 553–561.
13. Lartigue, A., P. Courville, I. Auquit, A. François, C. Arnoult, F. Tron, D. Gilbert, and P. Musette. 2006. Role of TLR9 in anti-nucleosome and anti-DNA antibody production in lpr mutation-induced murine lupus. *J. Immunol.* 177: 1349–1354.
14. Yu, P., U. Wellmann, S. Kunder, L. Quintanilla-Martinez, L. Jennen, N. Dear, K. Amann, S. Bauer, T. H. Winkler, and H. Wagner. 2006. Toll-like receptor 9-independent aggravation of glomerulonephritis in a novel model of SLE. *Int. Immunol.* 18: 1211–1219.
15. Nickerson, K. M., S. R. Christensen, J. Shupe, M. Kashgarian, D. Kim, K. Elkon, and M. J. Shlomchik. 2010. TLR9 regulates TLR7- and MyD88-dependent autoantibody production and disease in a murine model of lupus. *J. Immunol.* 184: 1840–1848.
16. Pan, Z. J., S. Maier, K. Schwarz, J. Azbill, S. Akira, S. Uematsu, and A. D. Farris. 2010. Toll-like receptor 7 (TLR7) modulates anti-nucleosomal autoantibody isotype and renal complement deposition in mice exposed to syngeneic late apoptotic cells. *Ann. Rheum. Dis.* 69: 1195–1199.
17. Santiago-Raber, M. L., I. Dunand-Sauthier, T. Wu, Q. Z. Li, S. Uematsu, S. Akira, W. Reith, C. Mohan, B. L. Kotzin, and S. Izui. 2010. Critical role of TLR7 in the acceleration of systemic lupus erythematosus in TLR9-deficient mice. *J. Autoimmun.* 34: 339–348.
18. Silver, K. L., T. L. Crockford, T. Bouriez-Jones, S. Milling, T. Lambe, and R. J. Cornall. 2007. MyD88-dependent autoimmune disease in Lyn-deficient mice. *Eur. J. Immunol.* 37: 2734–2743.
19. Pawar, R. D., P. S. Patole, D. Zecher, S. Segerer, M. Kretzler, D. Schlöndorff, and H. J. Anders. 2006. Toll-like receptor-7 modulates immune complex glomerulonephritis. *J. Am. Soc. Nephrol.* 17: 141–149.
20. Jackson, S. W., N. E. Scharping, N. S. Kolhatkar, S. Khim, M. A. Schwartz, Q. Z. Li, K. L. Hudkins, C. E. Alpers, D. Liggitt, and D. J. Rawlings. 2014. Opposing impact of B cell-intrinsic TLR7 and TLR9 signals on autoantibody repertoire and systemic inflammation. *J. Immunol.* 192: 4525–4532.
21. Meffre, E., and H. Wardemann. 2008. B-cell tolerance checkpoints in health and autoimmunity. *Curr. Opin. Immunol.* 20: 632–638.
22. Vinuesa, C. G., M. C. Cook, C. Angelucci, V. Athanasopoulos, L. Rui, K. M. Hill, D. Yu, H. Domaschenz, B. Whittle, T. Lambe, et al. 2005. A RING-type ubiquitin ligase family member required to repress follicular helper T cells and autoimmunity. *Nature* 435: 452–458.
23. Luzina, I. G., S. P. Atamas, C. E. Storrer, L. C. daSilva, G. Kelsoe, J. C. Papadimitriou, and B. S. Handwerger. 2001. Spontaneous formation of germinal centers in autoimmune mice. *J. Leukoc. Biol.* 70: 578–584.
24. Lee, S. K., D. G. Silva, J. L. Martin, A. Pratama, X. Hu, P. P. Chang, G. Walters, and C. G. Vinuesa. 2012. Interferon-γ excess leads to pathogenic accumulation of follicular helper T cells and germinal centers. *Immunity* 37: 880–892.
25. Linterman, M. A., R. J. Rigby, R. K. Wong, D. Yu, R. Brink, J. L. Cannons, P. L. Schwartzberg, M. C. Cook, G. D. Walters, and C. G. Vinuesa. 2009. Follicular helper T cells are required for systemic autoimmunity. *J. Exp. Med.* 206: 561–576.

26. Lamagna, C., Y. Hu, A. L. DeFranco, and C. A. Lowell. 2014. B cell-specific loss of Lyn kinase leads to autoimmunity. *J. Immunol.* 192: 919–928.
27. Simpson, N., P. A. Gatenby, A. Wilson, S. Malik, D. A. Fulcher, S. G. Tangye, H. Manku, T. J. Vyse, G. Roncador, G. A. Huttley, et al. 2010. Expansion of circulating T cells resembling follicular helper T cells is a fixed phenotype that identifies a subset of severe systemic lupus erythematosus. *Arthritis Rheum.* 62: 234–244.
28. Cappione, A., III, J. H. Anolik, A. Pugh-Bernard, J. Barnard, P. Dutcher, G. Silverman, and I. Sanz. 2005. Germinal center exclusion of autoreactive B cells is defective in human systemic lupus erythematosus. *J. Clin. Invest.* 115: 3205–3216.
29. Wong, E. B., T. N. Khan, C. Mohan, and Z. S. Rahman. 2012. The lupus-prone NZM2410/NZW strain-derived Sle1b sublocus alters the germinal center checkpoint in female mice in a B cell-intrinsic manner. *J. Immunol.* 189: 5667–5681.
30. William, J., C. Euler, S. Christensen, and M. J. Shlomchik. 2002. Evolution of autoantibody responses via somatic hypermutation outside of germinal centers. *Science* 297: 2066–2070.
31. Hwang, S. H., H. Lee, M. Yamamoto, L. A. Jones, J. Dayalan, R. Hopkins, X. J. Zhou, F. Yarovinsky, J. E. Connolly, M. A. Curotto de Lafaille, et al. 2012. B cell TLR7 expression drives anti-RNA autoantibody production and exacerbates disease in systemic lupus erythematosus-prone mice. *J. Immunol.* 189: 5786–5796.
32. Walsh, E. R., P. Pisitkun, E. Voynova, J. A. Deane, B. L. Scott, R. R. Caspi, and S. Bolland. 2012. Dual signaling by innate and adaptive immune receptors is required for TLR7-induced B-cell-mediated autoimmunity. *Proc. Natl. Acad. Sci. USA* 109: 16276–16281.
33. Hua, Z., A. J. Gross, C. Lamagna, N. Ramos-Hernández, P. Scapini, M. Ji, H. Shao, C. A. Lowell, B. Hou, and A. L. DeFranco. 2014. Requirement for MyD88 signaling in B cells and dendritic cells for germinal center anti-nuclear antibody production in Lyn-deficient mice. *J. Immunol.* 192: 875–885.
34. Hemmi, H., T. Kaisho, O. Takeuchi, S. Sato, H. Sanjo, K. Hoshino, T. Horiuchi, H. Tomizawa, K. Takeda, and S. Akira. 2002. Small anti-viral compounds activate immune cells via the TLR7 MyD88-dependent signaling pathway. *Nat. Immunol.* 3: 196–200.
35. Hemmi, H., O. Takeuchi, T. Kawai, T. Kaisho, S. Sato, H. Sanjo, M. Matsumoto, K. Hoshino, H. Wagner, K. Takeda, and S. Akira. 2000. A Toll-like receptor recognizes bacterial DNA. *Nature* 408: 740–745.
36. Morel, L., K. R. Blenman, B. P. Croker, and E. K. Wakeland. 2001. The major murine systemic lupus erythematosus susceptibility locus, Sle1, is a cluster of functionally related genes. *Proc. Natl. Acad. Sci. USA* 98: 1787–1792.
37. Rahman, Z. S., B. Alabyev, and T. Manser. 2007. FcgammaRIIB regulates autoreactive primary antibody-forming cell, but not germinal center B cell, activity. *J. Immunol.* 178: 897–907.
38. Shlomchik, M. J., and F. Weisel. 2012. Germinal centers. *Immunol. Rev.* 247: 5–10.
39. Zotos, D., and D. M. Tarlinton. 2012. Determining germinal centre B cell fate. *Trends Immunol.* 33: 281–288.
40. DeFranco, A. L., D. C. Rookhuizen, and B. Hou. 2012. Contribution of Toll-like receptor signaling to germinal center antibody responses. *Immunol. Rev.* 247: 64–72.
41. Meyer-Bahlburg, A., and D. J. Rawlings. 2008. B cell autonomous TLR signaling and autoimmunity. *Autoimmun. Rev.* 7: 313–316.
42. Sun, X., A. Wiedeman, N. Agrawal, T. H. Teal, L. Tanaka, K. L. Hudkins, C. E. Alpers, S. Bolland, M. B. Buechler, J. A. Hamerman, et al. 2013. Increased ribonuclease expression reduces inflammation and prolongs survival in TLR7 transgenic mice. *J. Immunol.* 190: 2536–2543.
43. Matzinger, P. 2002. The danger model: a renewed sense of self. *Science* 296: 301–305.
44. Avalos, A. M., L. Busconi, and A. Marshak-Rothstein. 2010. Regulation of autoreactive B cell responses to endogenous TLR ligands. *Autoimmunity* 43: 76–83.
45. Yu, P., W. Lübben, H. Slomka, J. Gebler, M. Konert, C. Cai, L. Neubrandt, O. Prazeres da Costa, S. Paul, S. Dehnert, et al. 2012. Nucleic acid-sensing Toll-like receptors are essential for the control of endogenous retrovirus viremia and ERV-induced tumors. *Immunity* 37: 867–879.
46. Giltiay, N. V., C. P. Chappell, X. Sun, N. Kolhatkar, T. H. Teal, A. E. Wiedeman, J. Kim, L. Tanaka, M. B. Buechler, J. A. Hamerman, et al. 2013. Overexpression of TLR7 promotes cell-intrinsic expansion and autoantibody production by transitional T1 B cells. *J. Exp. Med.* 210: 2773–2789.
47. Hardy, R. R., C. E. Carmack, S. A. Shinton, J. D. Kemp, and K. Hayakawa. 1991. Resolution and characterization of pro-B and pre-pro-B cell stages in normal mouse bone marrow. *J. Exp. Med.* 173: 1213–1225.
48. Allman, D., R. C. Lindsley, W. DeMuth, K. Rudd, S. A. Shinton, and R. R. Hardy. 2001. Resolution of three nonproliferative immature splenic B cell subsets reveals multiple selection points during peripheral B cell maturation. *J. Immunol.* 167: 6834–6840.
49. Wu, X., and S. L. Peng. 2006. Toll-like receptor 9 signaling protects against murine lupus. *Arthritis Rheum.* 54: 336–342.
50. Wandstrat, A. E., C. Nguyen, N. Limaye, A. Y. Chan, S. Subramanian, X. H. Tian, Y. S. Yim, A. Pertsemlidis, H. R. Garner, Jr., L. Morel, and E. K. Wakeland. 2004. Association of extensive polymorphisms in the SLAM/CD2 gene cluster with murine lupus. *Immunity* 21: 769–780.
51. Croker, B. P., G. Gilkeson, and L. Morel. 2003. Genetic interactions between susceptibility loci reveal epistatic pathogenic networks in murine lupus. *Genes Immun.* 4: 575–585.
52. Pisitkun, P., J. A. Deane, M. J. Difilippantonio, T. Tarasenko, A. B. Satterthwaite, and S. Bolland. 2006. Autoreactive B cell responses to RNA-related antigens due to TLR7 gene duplication. *Science* 312: 1669–1672.
53. Celhar, T., R. Magalhães, and A. M. Fairhurst. 2012. TLR7 and TLR9 in SLE: when sensing self goes wrong. *Immunol. Res.* 53: 58–77.
54. Hou, B., P. Saudan, G. Ott, M. L. Wheeler, M. Ji, L. Kuzmich, L. M. Lee, R. L. Coffman, M. F. Bachmann, and A. L. DeFranco. 2011. Selective utilization of Toll-like receptor and MyD88 signaling in B cells for enhancement of the antiviral germinal center response. *Immunity* 34: 375–384.
55. Hou, B., B. Reizis, and A. L. DeFranco. 2008. Toll-like receptors activate innate and adaptive immunity by using dendritic cell-intrinsic and -extrinsic mechanisms. *Immunity* 29: 272–282.
56. Browne, E. P. 2011. Toll-like receptor 7 controls the anti-retroviral germinal center response. *PLoS Pathog.* 7: e1002293.
57. Clingan, J. M., and M. Matloubian. 2013. B Cell-intrinsic TLR7 signaling is required for optimal B cell responses during chronic viral infection. *J. Immunol.* 191: 810–818.
58. Rookhuizen, D. C., and A. L. DeFranco. 2014. Toll-like receptor 9 signaling acts on multiple elements of the germinal center to enhance antibody responses. *Proc. Natl. Acad. Sci. USA* 111: E3224–E3233.
59. Cline, A. M., and M. Z. Radic. 2004. Murine lupus autoantibodies identify distinct subsets of apoptotic bodies. *Autoimmunity* 37: 85–93.
60. Neeli, I., M. M. Richardson, S. N. Khan, D. Nicolo, M. Monestier, and M. Z. Radic. 2007. Divergent members of a single autoreactive B cell clone retain specificity for apoptotic blebs. *Mol. Immunol.* 44: 1914–1921.
61. Herlands, R. A., S. R. Christensen, R. A. Sweet, U. Hershberg, and M. J. Shlomchik. 2008. T cell-independent and toll-like receptor-dependent antigen-driven activation of autoreactive B cells. *Immunity* 29: 249–260.
62. Groom, J. R., C. A. Fletcher, S. N. Walters, S. T. Grey, S. V. Watt, M. J. Sweet, M. J. Smyth, C. R. Mackay, and F. Mackay. 2007. BAFF and MyD88 signals promote a lupuslike disease independent of T cells. *J. Exp. Med.* 204: 1959–1971.
63. Fairhurst, A. M., S. H. Hwang, A. Wang, X. H. Tian, C. Boudreaux, X. J. Zhou, J. Casco, Q. Z. Li, J. E. Connolly, and E. K. Wakeland. 2008. Yaa autoimmune phenotypes are conferred by overexpression of TLR7. *Eur. J. Immunol.* 38: 1971–1978.
64. Mohan, C., E. Alas, L. Morel, P. Yang, and E. K. Wakeland. 1998. Genetic dissection of SLE pathogenesis. Sle1 on murine chromosome 1 leads to a selective loss of tolerance to H2A/H2B/DNA subnucleosomes. *J. Clin. Invest.* 101: 1362–1372.
65. Koh, Y. T., J. C. Scatizzi, J. D. Gahan, B. R. Lawson, R. Baccala, K. M. Pollard, B. A. Beutler, A. N. Theofilopoulos, and D. H. Kono. 2013. Role of nucleic acid-sensing TLRs in diverse autoantibody specificities and anti-nuclear antibody-producing B cells. *J. Immunol.* 190: 4982–4990.
66. Kono, D. H., M. K. Haraldsson, B. R. Lawson, K. M. Pollard, Y. T. Koh, X. Du, C. N. Arnold, R. Baccala, G. J. Silverman, B. A. Beutler, and A. N. Theofilopoulos. 2009. Endosomal TLR signaling is required for anti-nucleic acid and rheumatoid factor autoantibodies in lupus. *Proc. Natl. Acad. Sci. USA* 106: 12061–12066.
67. Desnues, B., A. B. Macedo, A. Roussel-Queval, J. Bonnardel, S. Henri, O. Demaria, and L. Alexopoulou. 2014. TLR8 on dendritic cells and TLR9 on B cells restrain TLR7-mediated spontaneous autoimmunity in C57BL/6 mice. *Proc. Natl. Acad. Sci. USA* 111: 1497–1502.
68. Umiker, B. R., S. Andersson, L. Fernandez, P. Korgaokar, A. Larbi, M. Pilichowska, C. C. Weinkauf, H. H. Wortis, J. F. Kearney, and T. Imanishi-Kari. 2014. Dosage of X-linked Toll-like receptor 8 determines gender differences in the development of systemic lupus erythematosus. *Eur. J. Immunol.* 44: 1503–1516.
69. Li, X., S. Jiang, and R. I. Tapping. 2010. Toll-like receptor signaling in cell proliferation and survival. *Cytokine* 49: 1–9.
70. Pone, E. J., J. Zhang, T. Mai, C. A. White, G. Li, J. K. Sakakura, P. J. Patel, A. Al-Qahtani, H. Zan, Z. Xu, and P. Casali. 2012. BCR-signalling synergizes with TLR-signalling for induction of AID and immunoglobulin class-switching through the non-canonical NF-κB pathway. *Nat. Commun.* 3: 767.
71. Kawai, T., and S. Akira. 2005. Toll-like receptor downstream signaling. *Arthritis Res. Ther.* 7: 12–19.